frontiers | Frontiers in Marine Science

TYPE Original Research
PUBLISHED 30 August 2023
DOI 10.3389/fmars.2023.1216564

OPEN ACCESS

EDITED BY
Peter Von Dassow,
Pontificia Universidad Católica de Chile, Chile

REVIEWED BY
Peter Vd'ačný,
Comenius University, Slovakia
Sergei Fokin,
University of Pisa, Italy

*CORRESPONDENCE
Jae-Ho Jung
jhjung@gwnu.ac.kr

RECEIVED 04 May 2023
ACCEPTED 18 July 2023
PUBLISHED 30 August 2023

CITATION
Quintela-Alonso P, Omar A, Moon JH and Jung J-H (2023) A new marine ciliate, *Apofrontonia jejuensis* n. sp. (Protozoa, Ciliophora, Oligohymenophorea) from Jeju Island, South Korea, and an improved diagnosis of the genus *Apofrontonia*. *Front. Mar. Sci.* 10:1216564.
doi: 10.3389/fmars.2023.1216564

A new marine ciliate, *Apofrontonia jejuensis* n. sp. (Protozoa, Ciliophora, Oligohymenophorea) from Jeju Island, South Korea, and an improved diagnosis of the genus *Apofrontonia*

Pablo Quintela-Alonso[1,2], Atef Omar[3], Ji Hye Moon[2] and Jae-Ho Jung[2*]

[1]Department of Genetics, Physiology and Microbiology, Faculty of Biology, Complutense University of Madrid, Madrid, Spain, [2]Department of Biology, Gangneung-Wonju National University, Gangneung, Republic of Korea, [3]Natural Science Research Institute, Gangneung-Wonju National University, Gangneung, Republic of Korea

The genus *Apofrontonia* comprises vicarious species that until now have only been described in a few locations worldwide. It was assigned to the family Frontoniidae based on two diagnostic features, i.e., the closely arranged kinetal rows in the peniculi and vestibular kineties on the right side of the vestibular cavity's opening. The first phylogenetic analysis of the genus was based on the 18S rRNA gene, and it was limited not only by the unavailability of other gene sequences from other species within the genus but also by the Peniculia in general. *Apofrontonia jejuensis* n. sp. was discovered in the coastal waters of Jeju Island, South Korea. Besides the genus-specific features, *A. jejuensis* n. sp. exhibits a fibrillar system associated with the oral ciliature, likely linked to nematodesmata-like structures, as seen in *Frontonia* species. This study increases the taxon sampling, offers further insights in the morphological variability of the genus *Apofrontonia*, and provides additional molecular support for its distinction from the genus *Frontonia*.

KEYWORDS

argyrophilic plate, morphology, nematodesmata-like fibres, phylogeny, postoral

Introduction

The genus *Apofrontonia* Foissner and Song, 2002, represents a group of peniculid ciliates that offers intriguing insights into the vicarious model of evolution, which posits that major biotic components evolve in tandem and are influenced by shared geographical and climatic fluctuations, offering insights into the formation of modern biogeographical

distributions. Vicarious species are characterized by their restricted geographical distribution, as they were geographically isolated *via* vicariance events, such as the emergence of natural barriers due to continental drift (Lincoln et al., 1982; Foissner et al., 2008). Although the three already known *Apofrontonia* species, namely, *Apofrontonia lametschwandtneri* Foissner and Song, 2002, *Apofrontonia dohrni* Fokin et al., 2006, and *Apofrontonia obtusa* (Song and Wilbert, 1989) Foissner and Song, 2002, exhibit notable similarities, they show restricted geographical distributions (Germany, Italy, and Venezuela) and live in slightly distinct habitats (mud from saline coastline puddles vs. freshwater ponds) (Song and Wilbert, 1989; Foissner and Song, 2002; Fokin et al., 2006). In this study, we contribute to the understanding of the genus, expanding our knowledge of its taxonomic diversity and evolutionary adaptations, by introducing a newly discovered species from Jeju Island, South Korea. Through the taxonomic and phylogenetic characterization of this South Korean *Apofrontonia* species, we offer valuable insights into its phylogenetic relationships, evolutionary history, and ecological niche, contributing to a broader understanding of the biogeography and significance of these peniculid ciliates.

According to Lynn (2008), the peniculi are a kind of oral polykinetids each composed of a long band of often short seemingly fused cilia. The infraciliary bases of peniculi typically consist of a variable number of closely arranged ciliary rows. Their presence is a major morphological feature defining the subclass Peniculia Fauré-Fremiet in Corliss, 1956, within the species-rich class Oligohymenophorea de Puytorac et al., 1974 (Kahl, 1931; Dragesco, 1960; Roque, 1961; Borror, 1963; Gil and Perez-Silva, 1964a, 1964b, 1964c; Dragesco, 1972; Roque and de Puytorac, 1972; Small and Lynn, 1985; Dragesco and Dragesco-Kernéis, 1986; Foissner et al., 1994; Song, 1995; Fokin et al., 2006; Lynn, 2008; Fan et al., 2011; Xu et al., 2018; Sun et al., 2020). Besides the oral apparatus, the somatic ciliature, the number of pores and collecting canals of the contractile vacuoles, and the number and shape of the macronuclear nodules are features used to characterize species within the morphologically well-defined group of peniculids (Foissner et al., 1994; Foissner and Song, 2002; Long et al., 2005; Fokin et al., 2006; Fokin, 2008; Long et al., 2008; Fan et al., 2011; Fan et al., 2013; Pan et al., 2013; Xu et al., 2018).

The systematics of the order Peniculida has changed in the last years, owing to new insights into their phylogenetic relationships (Xu et al., 2018; Serra et al., 2020; Sun et al., 2020; Serra et al., 2021; Serra et al., 2022), which recently caused a reduction in the number of families. Thus, the classification of the order Peniculida according to Lynn (2008), with its seven families, experienced three relevant modifications, i.e., (i) the transfer of the family Paranassulidae Fauré-Fremiet, 1962, from the class Nassophorea Small and Lynn, 1981, by Gao et al. (2016); (ii) the synonymization of the Maritujidae Jankowski in Small and Lynn, 1985, with the Stokesiidae Roque, 1961, as proposed by Xu et al. (2018); and (iii) the withdrawal of the family Neobursaridiidae Dragesco and Tuffrau, 1967, as its only genus, *Neobursaridium* Balech, 1941, has been recently transferred to the family Parameciidae Dujardin, 1840, becoming a subgenus of *Paramecium* Müller, 1973 (Serra et al., 2020, 2022). Accordingly, the order Peniculida currently includes six families: the Clathrostomatidae Kahl, 1926; Frontoniidae Kahl, 1926; Lembadionidae Jankowski in Corliss, 1979; Parameciidae Dujardin, 1840; Paranassulidae Gao et al., 2016; and Stokesiidae Roque, 1961.

Unfortunately, many phylogenetic relationships within the order Peniculida are still unsolved due to the limited and unbalanced taxon sampling, i.e., molecular data in GenBank currently include only representatives from five out of the six peniculid families, while data for the family Clathrostomatidae Kahl, 1926, are currently missing. Moreover, most of the peniculid sequences available from GenBank belong to *Frontonia* Ehrenberg, 1838, and *Paramecium* species, while other genera, such as *Apofrontonia*, *Clathrostoma* Penard, 1922, *Disematostoma* Lauterborn, 1894, and *Marituja* Gajewskaja, 1928, are underrepresented.

Foissner and Song (2002) established the genus *Apofrontonia* based on a combination of three features, *viz.*, (i) a pyriform vestibular opening occupying more than half of the body length; (ii) a bowl-shaped vestibulum that posteriorly gradually merges into the cell surface, completely exposing three similarly structured peniculi; and (iii) many (>6) vestibular kineties covering the sigmoidal right vestibular wall and not extending beyond the oral cavity. Thereby, *A. lametschwandtneri* and *A. obtusa* (basionym: *Frontonia obtusa*) could be distinguished from other peniculines mainly by their large oral apparatuses. The authors suggested an affiliation of the genus *Apofrontonia* with the family Frontoniidae because it possesses (i) three similarly structured peniculi (vs. quadrulus in *Paramecium*, *Stokesia* Wenrich, 1929, and *Neobursaridium*), (ii) basically frontoniid vestibular kineties (vs. absent in *Lembadion* Perty, 1849, *Urocentrum* Nitzsch, 1827, *Paramecium*, and *Neobursaridium*), and (iii) a pyriform vestibular opening more similar to the triangular one of *Frontonia* (vs. bursiform or oval in *Paramecium*, *Neobursaridium*, *Stokesia*, *Lembadion*, and *Urocentrum*). Subsequent studies by Fokin et al. (2006) and Xu et al. (2018) showed that *Apofrontonia* differs from the other genera of the Frontoniidae, particularly *Marituja* or *Disematostoma*, in the supposed lack of the most permanent features of frontoniids according to Lynn and Small (2000), namely, the oral nematodesmata and the vestibular kineties extending across one-third to one-half of body length. Fokin et al. (2006) argued that both morphological and molecular data justify the removal of *Apofrontonia* from the Frontoniidae and potentially the establishment of a distinct family in the Peniculida. Due to the limited number of available 18S rRNA gene sequences from related genera and families, however, the genus was provisionally placed as incertae sedis in the Peniculida. Some years later, Xu et al. (2018) analyzed the phylogenetic relationships among the Peniculida. Despite the absence of a synapomorphy, the close relationship of *Apofrontonia* and *Frontonia* in the molecular trees was used to assign the genus *Apofrontonia* again to the family Frontoniidae, as proposed by Foissner and Song (2002). Moreover, Xu et al. (2018) regarded the similarities between *Apofrontonia* and *Marituja* concerning cell shape, large vestibulum, increased number of vestibular kineties, and sausage-shaped macronucleus (Foissner and Song, 2002; Fokin et al., 2006; Xu et al., 2018) as homoplasious features.

In the present study, we provide the morphological and molecular description of a new marine *Apofrontonia* species collected from the coast of Jeju Island, South Korea, improving the genus diagnosis and increasing the taxon sampling within the non-monophyletic family Frontoniidae.

Materials and methods

Sampling site and cell culture

A water sample including debris was collected using a plastic bottle (500 mL) from Jeongju Port, Jeju-si, Jeju-do, Republic of Korea (33°32'49"N, 126°39'36"E) on 20 May 2020. The sample was obtained after stirring the bottom sediment composed of sand and shells of clams and sea urchins and collecting the mixture together with seawater at a depth of 20–30 cm. The salinity and the temperature of the water sample were 30.6‰ and 20.7°C, respectively. The sample was kept in a plant culture dish (SPL Lifesciences, Gyeonggido, Korea; 100 mm across × 40 mm deep) at room temperature (20°C), and few wheat grains were added to promote the growth of bacteria as food resource. The absence of other peniculid species in the preparations prevented the misidentification of *Apofrontonia* n. sp., even though we were unable to establish clonal cultures.

Morphological methods

Living specimens were investigated using a stereomicroscope (Olympus SZ61, Japan) and a light microscope (Olympus BX53) with differential interference contrast at 50–1,000× magnification. The ciliary pattern was revealed by protargol, silver carbonate (not used for measurements), wet silver nitrate impregnation, and scanning electron microscopy (SEM). The protargol powder was synthesized following Kim and Jung (2017). The protargol impregnation technique is based on "procedure A" of Foissner (1991, 2014); the silver carbonate and wet silver nitrate stainings follow Foissner (1991, 2014). The shape and position of the nuclear apparatus was determined by staining formalin-fixed cells for 10 min in 4'-6-diamidino-2-phenylindole (DAPI; 0.1 μg mL^{-1} final concentration) and observing them by means of an Olympus BX53 microscope fitted with a U-RFL-T epifluorescence attachment, a U-LH100HG fluorescence light source, and an Olympus DP74 digital camera. SEM was conducted following the procedure of Foissner (2014) and Moon et al. (2020) using a scanning electron microscope (Jeol JSM-IT500, Japan). The terminology is according to Lynn (2008), except for the term "postoral kinety," which refers to ciliary rows that are anteriorly shortened and thus do not commence at the left side of the preoral suture, in accordance with Foissner and Song (2002). The staining methods used in our study revealed a fibrillar system associated with the oral apparatus, which is most likely representative of nematodesmata. However, since an ultrastructural analysis of these argyrophilic structures has not yet been conducted, it is uncertain whether they are homologous to the distinctive nematodesmata found in the oral ciliature of *Frontonia* spp. For this reason, in this study, the term "nematodesmata-like fibers" is used to refer to these argyrophilic structures. Both peniculus 1 and the vestibular opening are approximately of the same length, which is convenient for morphometric data collection.

DNA extraction, PCR amplification, and sequencing

Five cells were collected from the raw culture using a microcapillary under the stereomicroscope. The cells were washed using sterile seawater at least five times to remove other eukaryotes and then transferred with a minimum of water to a 1.5-mL centrifuge tube each. The genomic DNA was extracted using a RED-Extract-N-Amp Tissue PCR Kit (Sigma, St. Louis, MO, USA). The 18S rRNA gene was amplified using the primer New Euk A (5′-CTG GTT GAT YCT GCC AGT-3′) (Jung and Min, 2009), which is a slightly modified version of the primer Euk A in Medlin et al. (1988), and Euk B (5′-TGA TCC TTC TGC AGG TTC ACC TAC-3′). The PCR conditions were as follows: denaturation at 94°C for 90 s, followed by 40 cycles of denaturation at 98°C for 10 s, annealing at 58.5°C for 30 s, extension at 72°C for 2 min, and a final extension step at 72°C for 7 min. For purification of the PCR products, MEGAquickspin Total Fragment DNA Purification Kit (iNtRON, South Korea) was used. Since the sequence fragments of the five cells determined by the New Euk A were completely identical, we completed the sequencing from only one cell using the reverse primer and two internal primers, 18SR300 and 18SF790v2 (Park et al., 2017; Jung et al., 2018). DNA sequencing was performed using an ABI 3700 sequencer (Applied Biosystems, Foster City, CA, USA).

Phylogenetic analyses

The 18S rRNA gene sequence of *A. jejuensis* n. sp. was assembled using Geneious 9.1.5 (Kearse et al., 2012). The 18S rRNA gene dataset consists of 60 sequences including *A. jejuensis* n. sp., *Paramecium* (*Neobursaridium*) *gigas*, and an outgroup comprising two *Lembadion* species. The alignment was done using ClustalW (Thompson et al., 1994), and both ends were manually trimmed in BioEdit 7.2.5 (Hall, 1999). The optimal substitution model GTR+I+Γ was selected with jModelTest 2.1.10 (Darriba et al., 2012) according to the Akaike information criterion (AIC). The maximum likelihood (ML) tree was constructed using IQ-Tree 1.6.11 (Nguyen et al., 2015). The reliability of internal branches was assessed using a standard nonparametric bootstrap method with 1,000 replicates. The pairwise distances and the number of nucleotide differences among the taxa were calculated in Mega 6.06 (Tamura et al., 2013) using the p-distance method. MrBayes 3.2.6 (Ronquist et al., 2012) was used for Bayesian inference (BI) analyses with Markov chain Monte Carlo for 3,000,000 generations with a sampling frequency of every 100 generations, and the first 7,500 trees were discarded as burn-in. The phylogenetic trees were visualized using the free software package FigTree v1.4.4 by Rambaut (2006).

Results

ZooBank registration

Present work: urn:lsid:zoobank.org:pub:5C729BA6-A422-48C2-A199-B6E1CD497097

Apofrontonia jejuensis n. sp.: urn:lsid:zoobank.org:act:94248C8C-3B96-4BE0-8326-343C1EA08220.

Taxonomy

Class Oligohymenophorea de Puytorac et al., 1974
Subclass Peniculia Fauré-Fremiet in Corliss, 1956
Order Peniculida Fauré-Fremiet in Corliss, 1956
Family Frontoniidae Kahl, 1926
Genus *Apofrontonia* Foissner and Song, 2002

Improved diagnosis

Medium-sized (80–200 µm) Frontoniidae with large oral apparatus occupying at least approximately 40% of the ventral side. Numerous (between 5 and 30) contractile vacuoles randomly situated beneath the body surface. Macronucleus sausage-shaped. Up to three micronuclei, usually one. Vestibular cavity with bean-, pyriform-, or keyhole-shaped opening, bowl-shaped and posteriorly gradually merging into the cell surface, completely exposing three similarly structured comparatively large peniculi. Right vestibular wall more or less sigmoidal, covered by a variable number (≥3) of vestibular kineties usually not extending beyond the vestibular cavity. Postoral field distinct to highly reduced with postoral kineties variable in presence and number. Argyrophilic plate of nematodesmata-like fibers between paroral membrane and cytostome recognizable in some species. Species distributed in a wide range of salinities, including fresh, brackish, and marine waters, and soil habitats.

Apofrontonia jejuensis n. sp.

Diagnosis

Cell approximately 92 × 50 µm *in vivo*, usually oval to broadly elliptical in dorsal and ventral view, somewhat dorsoventrally flattened. Rightmost vestibular kinety extends beyond the vestibular cavity, occupies up to 50% of body length. Pellicular ridges (oral ribs) on the right vestibular wall, between paroral membrane and cytostome, underlaid by an argyrophilic fibrous plate. Preoral and postoral sutures distinct, somewhat extending onto the dorsal side; preoral suture comparatively short. Macronucleus in the middle third of the cell, sausage-shaped, sometimes tortuous; up to three globular micronuclei. Approximately 20 contractile vacuoles. On average, 78 somatic, 5 postoral, and invariably 3 vestibular kineties. Peniculi 1, 2, and 3 composed of invariably 7, 6, and 3 ciliary rows, respectively.

Type locality

Coastal waters of Jeju Island, Jeju Province, South Korea (33° 32.817′N, 126°39.600′E).

Type materials

The slide containing the holotype (MABIK PR3549) plus protargol-impregnated paratype specimens has been deposited in the National Marine Biodiversity Institute of Korea (MABIK), South Korea. Additional six paratype slides (protargol preparations: GUC003551, 3554, 3562, 3564; wet silver nitrate preparations: GUC003558, 3559) have been deposited in the Jung-lab (J-HJ) in Gangneung-Wonju National University.

Etymology

Named after Jeju Island, South Korea, where the new species had been discovered.

Gene sequence

The 18S rRNA gene sequence of *A. jejuensis* n. sp. has been deposited in GenBank under the accession number OP798095 (1,728 base pairs long and 44.38% GC content).

Morphological description

Size *in vivo* 80–105 × 39–63 µm, on average 92 × 50 µm, depends on the fixative and silver staining method used, *viz.*, 58–86 × 43–54 µm (78 × 49 µm on average) after ethanol + protargol staining; 91–111 × 59–86 µm (101 × 73 µm on average) after Stieve's fluid + protargol; and 102–121 × 89–100 µm (113–95 µm on average) after Champy's fixative + "wet" silver nitrate. Length:width ratio 1.3–1.5 *in vivo* (1.4 on average) while slightly deformed in preparations, i.e., 1.46–1.76 after ethanol + protargol, 1.19–1.53 after Stieve's fluid, and 1.16–1.28 after Champy's fixative + "wet" silver nitrate (Table 1). Body outline oval to broadly elliptical, slightly obovate in some specimens; in cross section, circular to broadly elliptical due to slight dorsoventral flattening. Anterior end slightly more broadly rounded than posterior end, smoothly rounded or slightly tapering, particularly noticeable in preparations; cells somewhat flexible, but hardly contractile, tend to become circular in disturbed and in preserved specimens (Figures 1A, D–G, 2A, 3A–F, 4A–D). Macronucleus in middle third of cell, frequently extending posteriad; sausage-shaped, sometimes tortuous, approximately 125 µm long, with slightly inflated rounded ends, which may appear somewhat pointed (Figures 1A, D–G, 2A, 3I, 4A, B, 5D; Table 1). One to three globular micronuclei approximately 2.6 µm across, distant from macronucleus, i.e., usually subterminal (Figures 1A, D–G, 2A, 3I; Table 1). Approximately 20 contractile vacuoles, mainly scattered in cell periphery of the dorsal side; a single, rarely two, excretory pore for each contractile vacuole between ciliary rows (Figures 1A, 3E, 4D, E, 6D). Cytopyge slit-like, extends in the posterior ventral portion of the postoral suture. Cortex composed of ordinary peniculine units, i.e., quadrangular meshes with one or two strongly impregnated basal bodies and one parasomal sac (Figures 3A, D, 4C–E, 6B–D; note that two out of the three parasomal sac-like structures in Figure 6D might be deciliated basal bodies). Kinetodesmal fibers associated with the basal bodies extend anteriorly on the right side of each kinety (Figures 4A, B). Extrusomes (trichocysts)

10.3389/fmars.2023.1216564

TABLE 1 Morphometric data on *Apofrontonia jejuensis* n. sp. from Jeju Island, South Korea.

Characteristic[a]	Method	Min	Max	Mean	M	SD	SE	CV	n
Body, length	LO	80.0	105.0	91.6	91.0	7.4	1.9	8.1	15
	E	57.7	86.1	78.5	79.2	5.5	1.0	7.0	31
	S	90.9	111.1	101.3	101.7	5.2	1.3	5.1	16
	WSN	102.2	121.0	112.8	113.5	4.8	1.3	4.2	14
Body, width in ventral and dorsal view	LO	39.0	63.0	49.8	48.0	6.7	1.7	13.5	15
	E	43.5	53.6	49.1	49.2	3.0	0.7	6.1	16
	S	59.4	86.2	72.9	71.3	8.4	2.2	11.5	14
	WSN	89.5	99.6	94.9	96.9	4.2	1.9	4.5	5
Body, thickness	E	37.7	52.9	48.5	48.4	4.0	1.1	8.2	14
	WSN	72.9	94.4	87.6	89.0	6.6	2.3	7.6	8
Body length:width, ratio in ventral and dorsal view	E	1.46	1.76	1.61	1.60	0.10	0.02	6.0	16
	S	1.19	1.53	1.40	1.44	0.11	0.03	7.9	14
	WSN	1.16	1.28	1.24	1.24	0.05	0.02	3.8	5
Body length:thickness, ratio in lateral view	E	1.43	1.76	1.60	1.63	0.11	0.03	6.6	14
	WSN	1.23	1.40	1.28	1.27	0.05	0.02	4.2	8
Anterior body end to peniculus 1, distance	E	0.6	8.4	4.2	4.0	2.1	0.4	51.1	29
	S	0.0	7.5	2.4	1.4	2.5	0.7	105	14
Anterior body end to posterior end of peniculus 1, distance	E	31.8	44.6	36.9	37.1	3.3	0.6	8.9	29
	S	38.1	47.8	43.3	43.6	3.4	0.9	7.8	13
Posterior end of peniculus 1 to posterior body end, distance	E	25.6	48.3	41.4	41.8	4.7	0.9	11.5	29
	S	45.0	71.5	57.5	56.7	6.9	1.9	12.0	13
Cytostome, length	WSN	24.1	27.9	24.9	24.3	1.4	0.5	5.5	7
	S	22.7	28.6	27.2	27.6	1.8	0.6	6.5	10
Body length:cytostome length, ratio	WSN	4.1	4.7	4.5	4.5	0.2	0.1	5.6	7
	S	3.2	4.4	3.7	3.8	0.3	0.1	8.7	10
Vestibular cavity, maximum width	E	9.1	11.5	10.4	10.4	0.7	0.2	6.4	16
	S	11.4	17.8	15.3	15.1	2.0	0.5	13.2	15
Peniculus 1, length	E	30.5	36.3	32.8	33.1	1.4	0.3	4.3	29
	S	36.9	47.8	41.3	40.8	2.7	0.7	6.5	14
Peniculus 2, length	S	36.7	45.1	39.8	39.4	2.5	0.7	6.2	14
Peniculus 3, length	E	21.4	24.4	23.4	23.9	1.2	0.5	5.1	5
	S	24.9	30.1	27.7	28.2	1.7	0.4	6.0	15
Macronucleus, length	S	72.3	158.3	125.2	126.0	22.9	5.3	18.3	19
Macronucleus, width	S	4.1	7.4	5.9	6.0	0.9	0.2	14.4	19
Micronuclei, number	E	1.0	3.0	1.9	2.0	0.7	0.2	37.0	17
Micronucleus, diameter	E	1.7	3.4	2.6	2.6	0.4	0.1	16.5	17
Peniculus 1, number of ciliary rows	S	7.0	7.0	7.0	7.0	0.0	0.0	0.0	19
Peniculus 2, number of ciliary rows	S	6.0	6.0	6.0	6.0	0.0	0.0	0.0	19
Peniculus 3, number of ciliary rows	S	3.0	3.0	3.0	3.0	0.0	0.0	0.0	19

(Continued)

TABLE 1 Continued

Characteristic[a]	Method	Min	Max	Mean	M	SD	SE	CV	n
Vestibular kineties, number	E	3.0	3.0	3.0	3.0	0.0	0.0	0.0	20
	S	3.0	3.0	3.0	3.0	0.0	0.0	0.0	14
Postoral kineties, number	E	2.0	8.0	5.2	5.0	1.4	0.3	27.6	19
	S	3.0	9.0	5.2	5.0	1.5	0.5	29.7	11
Somatic kineties, number	E	75.0	82.0	78.1	78.0	1.8	0.4	2.3	16

[a]Data based, if not mentioned otherwise, on protargol-impregnated specimens; all measurements in µm.
CV, coefficient of variation (%); E, ethanol-fixed cells; LO, live observation; M, median; Max, maximum; mean, arithmetic mean; Min, minimum; n, number of specimens examined; S, Stieve-fixed cells; SD, standard deviation; SE, standard error of arithmetic mean; WSN, Champy's fixative + wet silver nitrate.

numerous, regularly arranged, i.e., alternate with somatic kineties, ellipsoidal to elongate ovoidal approximately 3–4 × 1 µm in size, slightly asymmetrical in resting state; in extruded state, up to 13 × 0.4 µm long, drumstick-shaped, and slightly curved with a more or less elongated filiform end (Figures 1B, C, 3H, 5D–G). Cell colorless to opaque because of densely arranged extrusomes. Cytoplasm contains lipid droplets up to 5 µm across, some crystals 1–3 µm in size, and food vacuoles up to 25 µm across (Figures 1A, 3B–D, F); probably feeds on different microorganisms, including bacteria, small diatoms, and small ciliates. Cells glide and swim rather fast by rotation about main body axis, particularly when disturbed, remain almost motionless while feeding. No cysts were observed.

Somatic cilia approximately 8 µm long *in vivo*, arranged in 75–82 narrowly spaced rows, less than 2 µm apart (Figures 1A, 2A, 3G, 4A, B, 5A, 6A; Table 1). Preoral and postoral sutures distinct, extend somewhat onto the dorsal side; preoral suture rather short on the ventral side due to the position of the vestibular cavity in anterior third of the cell (Figures 2A, C, D, 4A–C, 5A–C, H, J). Ciliary rows meridional, those on the dorsal side extend between preoral and postoral suture (Figures 1A, 2A, 4A, 5A, B, H–J; Table 1).

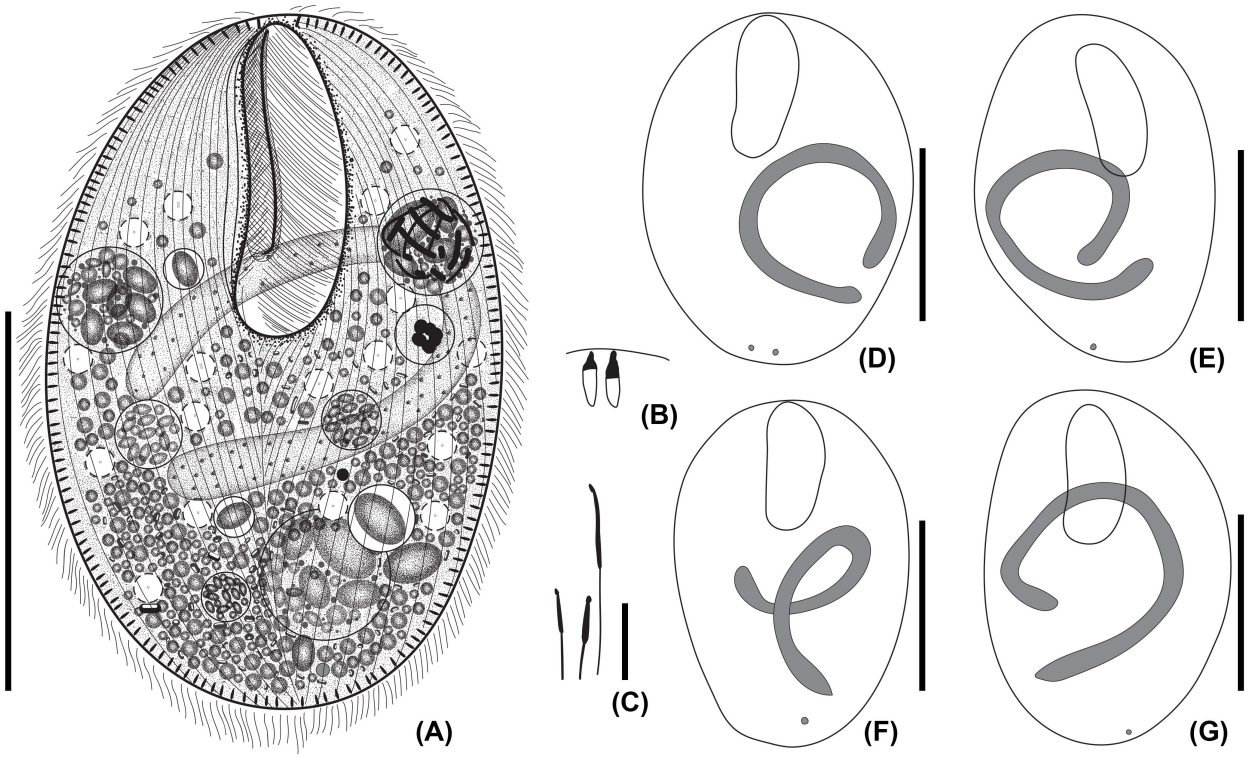

FIGURE 1
Apofrontonia jejuensis n. sp. from life **(A)** and after protargol staining **(B–G)**. **(A)** Ventral view of a representative specimen. **(B)** Extrusomes in resting state slightly asymmetrical, ellipsoidal to narrowly ovate extrusomes beneath the pellicle, approximately 3–4 × 1 µm in size. **(C)** Ejected extrusomes approximately 13 × 0.4 µm long, become drumstick-shaped and slightly bent with a filiform portion. **(D–G)** Shape variability of body, vestibular opening, and the sausage-shaped macronucleus, which is sometimes tortuous with slightly inflated rounded ends, which in some specimens may look somewhat pointed. The usually single globular micronucleus is distinctly apart from the macronucleus and subterminal. Scale bars: 50 µm **(A, D–G)** and 5 µm **(B, C)**.

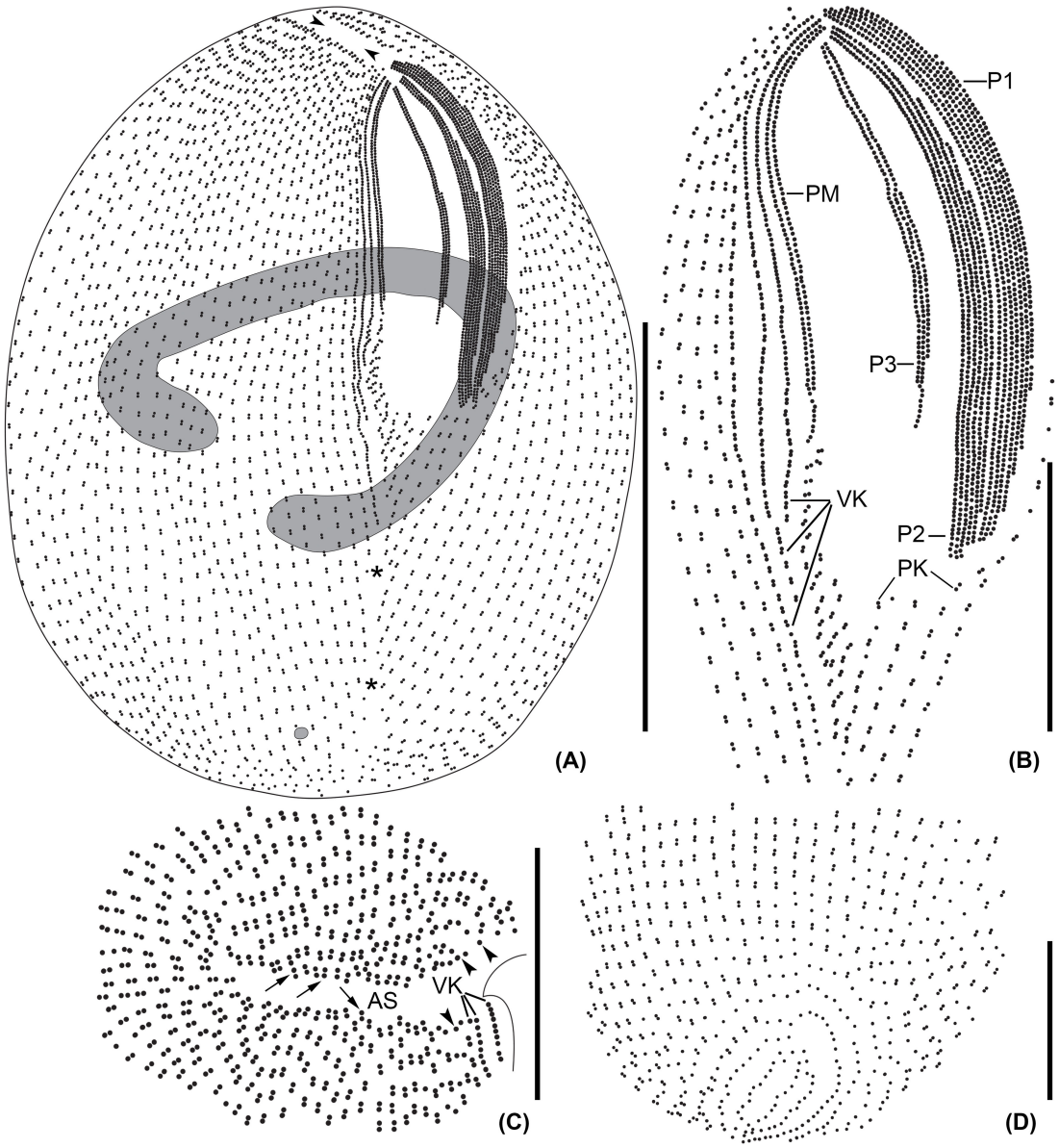

FIGURE 2
Line diagrams of *Apofrontonia jejuensis* n. sp. after protargol impregnation. **(A)** Ventrolateral view of the holotype specimen showing the somatic and oral ciliary pattern and the nuclear apparatus. Note the preoral (arrowheads) and postoral sutures (asterisks). **(B)** Detail of the buccal area. The three peniculi (P1–3) extend across the left vestibular wall. Three vestibular kineties extend along the right vestibular margin, the rightmost one extending beyond the vestibular cavity. Note the triangular postoral field at the posterior vertex of the vestibular opening, covered by a disorganized field of dikinetids following the posterior end of the paroral membrane and along the posterior end of the right vestibular wall, and the short postoral kineties abutting on the postoral suture. **(C)** Apical view showing the preoral suture and the anterior end of the ciliary rows either having a dikinetid (arrows) or probably a monokinetid (arrowheads). **(D)** Dorsal view of posterior body end showing the posterior end of the ciliary rows abutting on the postoral suture. AS, anterior (preoral) suture; P1, 2, 3, peniculi; PM, paroral membrane; PK, postoral kineties; VK, vestibular kineties. Scale bars: 50 µm **(A)**, 20 µm **(B)**, and 15 µm **(C, D)**.

Vestibular opening occupies approximately 40% of the body length and up to 20% of the body width, subapical (on average 4.2 µm apart from anterior end), bean-shaped, i.e., left margin convex, right margin almost straight to sigmoidal; anterior end more narrowly rounded than posterior end, slightly acute in some specimens (Figures 1A, D–G, 2A, 3A–D, F, 4A, C, 5A, 6A, B; Table 1). Vestibular cavity deepest in anterior half (Figures 6A, B, 7A). Left vestibular wall covered by the three peniculi (P1–3), right vestibular wall bears invariably three vestibular kineties and a paroral membrane (Figures 2A, B, 3A, C, 4A, C, 5A, H–J, 6A, B, 7A, B; Table 1). Vestibular kineties composed of densely spaced dikinetids, rightmost kinety extends beyond the vestibular cavity, abutting on the postoral suture, the two remaining kineties gradually shortened from right to left (Figures 2A, B, 4A, C, 5A, H–J, 6A, 7A). Paroral membrane on the left side of vestibular kineties, composed of two parallel rows of closely spaced basal bodies, left row shortened posteriorly (Figures 2A, B, 4A, C, 5A, H–J, 7A, B). The postoral field commences posterior to the peniculi

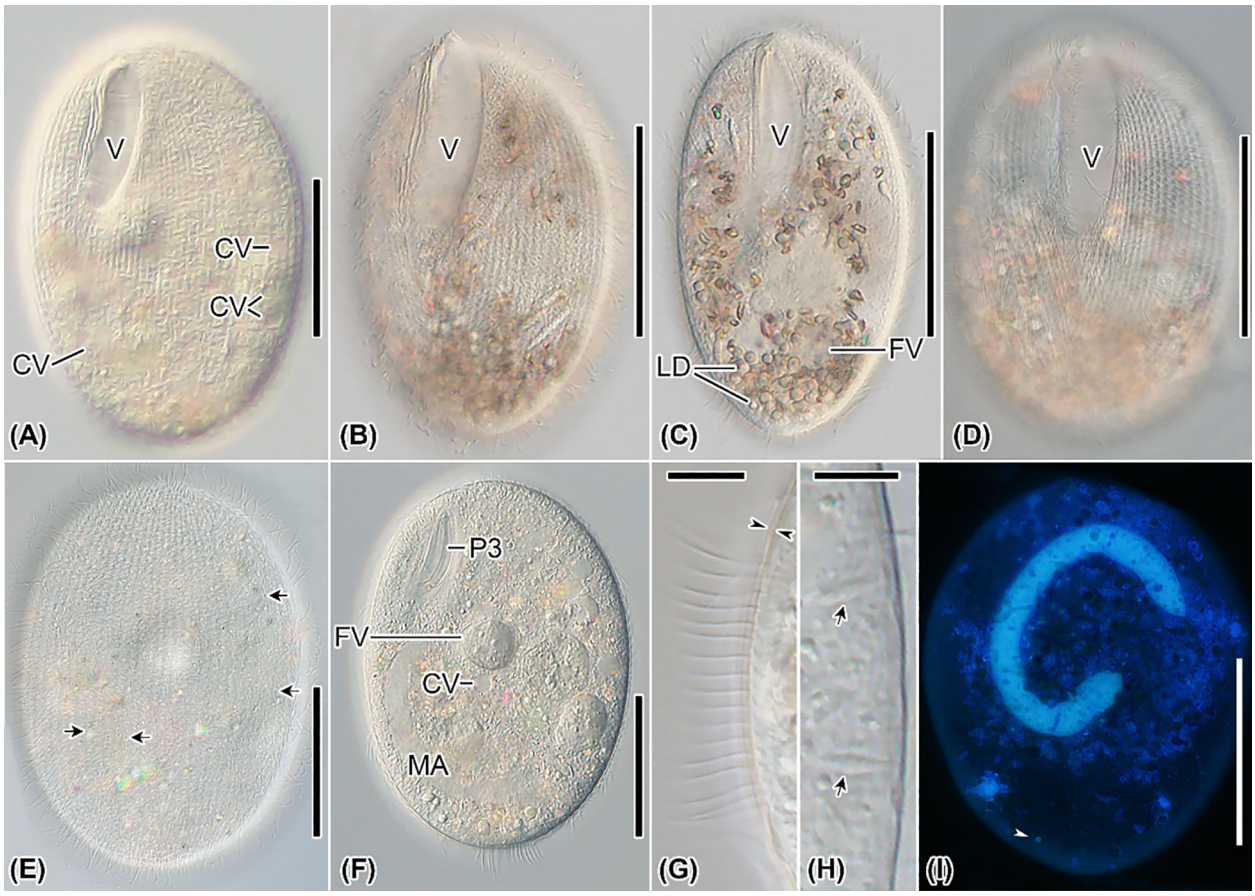

FIGURE 3
Apofrontonia jejuensis n. sp. from life **(A–H)** and after DAPI **(I)**. **(A–F)** Ventrolateral **(A, B, F)**, slightly ventrolateral **(C)**, ventral **(D)**, and dorsal **(E)** views of specimens under differential interference contrast optics. The excretory pores (arrows in **E**) of the contractile vacuoles **(A, F)** are mainly on the dorsal side. Specimens are packed with lipid droplets and food vacuoles mainly in the posterior third of the cell **(B–D, F)**. **(G)** Optical section of the cortex (opposed arrowheads) showing the somatic cilia approximately 10 µm long. **(H)** Optical section of the cell periphery showing the fusiform extrusomes (arrows). **(I)** Ventral view showing the nuclear apparatus, composed of a sausage-shaped macronucleus and a subterminal micronucleus (arrowhead). CV, contractile vacuole; FV, food vacuoles; LD, lipid droplets; MA, macronucleus; P3, peniculus 3; PM, paroral membrane; V, vestibulum. Scale bars: 50 µm **(A–F, I)**, 8 µm **(G)**, and 5 µm **(H)**.

and the paroral membrane, bears irregularly arranged dikinetids on right half and approximately five postoral kineties on left half gradually increasing in length to left; both the irregularly arranged dikinetids and kineties are obliquely arranged rightward (Figures 2A, B, 5A, H–J). P1 almost as long as P2 (41 µm vs. 40 µm on average in protargol-stained cells after Stieve's fluid fixation) and vestibulum, slightly narrowed anteriorly and posteriorly due to shortened left kineties. P1 composed of invariably seven rows of regularly and densely spaced kinetids, each bearing a cilium (Figures 2A, B, 5H–J, 7A, B; Table 1); cilia in P1 gradually decrease from 8–10 µm in middle portion to approximately 3 µm in both peniculi ends; P2 close to P1, composed of invariably six rows of regularly and densely spaced cilia and with a navicular outline, that is, distinctly narrowed anteriorly as the three leftmost rows are gradually shortened anteriorly and posteriorly (Figures 2A, B, 4A, B, 5H–J, 7A, B; Table 1); P3 somewhat separated from P2 and approximately 40% shorter (27.7 µm long on average in protargol-stained cells after Stieve's fluid fixation), composed of invariably three rows of closely spaced cilia 5–6 µm long (Figures 2A, B, 4A, B, 5H–J, 7A, B; Table 1). Cytostome separated from the paroral membrane by clockwise inclined pellicular ridges (oral ribs), which extend in upper right to lower left direction, until abutting on the sigmoidal cytostome slit at 45° angles. Similar but shorter ridges extend as a mirror image, i.e., from lower right to upper left at 45° angles, garnishing the left margin of the cytostome slit until next to P3 (Figures 4A, 5A, H–J, 7B). Argyrophilic fibrous plates of widely spaced nematodesmata-like fibers subjacent distal ends of the pellicular ridges converge and plunge into cytoplasm (Figures 5H–J, 6B, 7A, B).

Occurrence and ecology

Apofrontonia jejuensis n. sp. was so far only found at the type location. The sample where it was discovered consisted of a mixture of the stirred bottom sediment composed of sand and shells of clams and sea urchins and seawater with a salinity of 30.6‰ and a temperature of 20.7°C. *Apofrontonia jejuensis* n. sp. feeds on different microorganisms, likely including bacteria, small diatoms, and small-sized ciliates, as inferred from the food vacuoles' content.

10.3389/fmars.2023.1216564

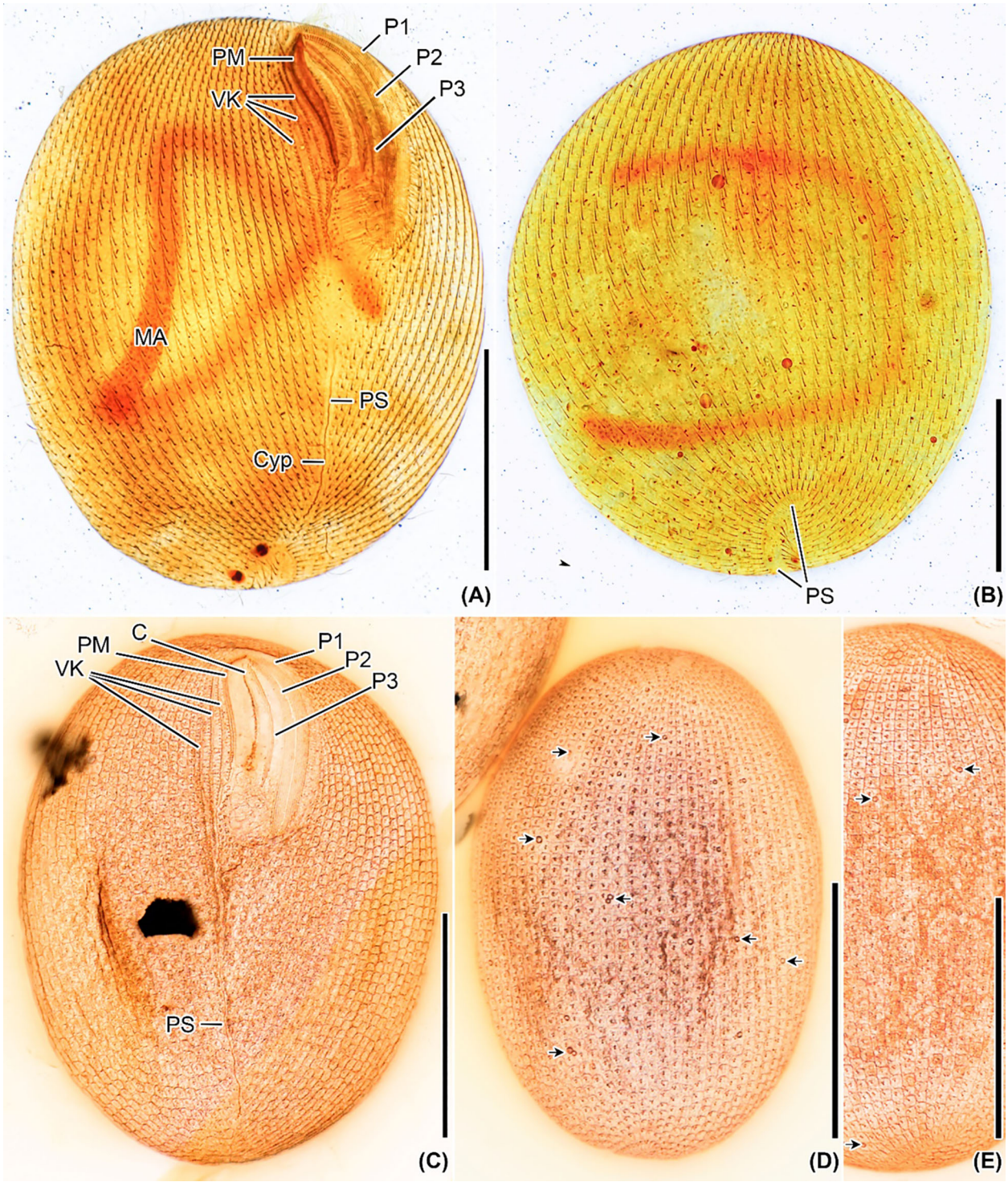

FIGURE 4
Apofrontonia jejuensis n. sp. after silver carbonate **(A, B)** and wet (Chatton–Lwoff) silver nitrate **(C–E)** impregnation. **(A, B)** Ciliary patterns of the ventrolateral **(A)** and dorsal side **(B)** showing the three large peniculi and the paroral membrane. Note the long sausage-shaped macronucleus and the ciliary rows abutting on the postoral suture, which extends to the posterior pole and ends subterminally on the dorsal side. The lack of some basal bodies on the dorsal side is due to staining artifact. **(C–E)** Argyrome of the ventral **(C)** and dorsal sides **(D, E)**. Ordinary peniculine units, i.e., quadrangular meshes with one, two, or even three strongly impregnated basal bodies forming triangles and one parasomal sac. Excretory pores of the contractile vacuoles are between the ciliary rows (arrows) **(D, E)**. C, cytostome; Cyp, cytopyge; MA, macronucleus; P1, 2, 3, peniculi; PM, paroral membrane; PS, postoral suture; VK, vestibular kineties. Scale bar: 50 µm.

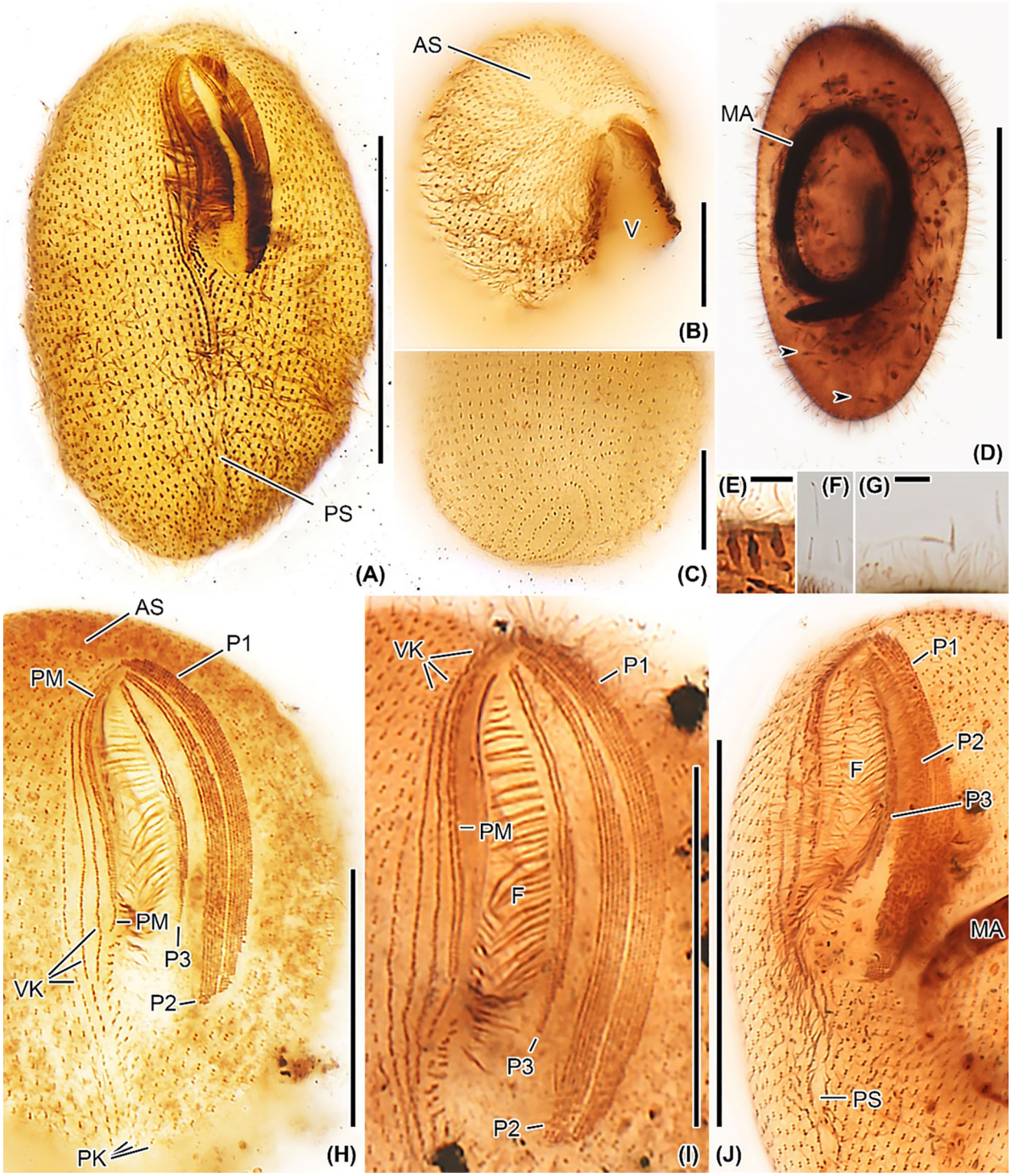

FIGURE 5
Apofrontonia jejuensis n. sp. after protargol impregnation. **(A)** Ventral view showing the oral and somatic ciliature. **(B)** Oblique apical view showing the rather short preoral suture formed by the anterior ends of the somatic ciliary rows. The anterior end of the vestibular area might be slightly acute in some specimens. **(C)** Oblique view of the posterior pole area showing the dorsal portion of the postoral suture. The posterior ends of the ciliary rows abut on the postoral suture, creating an elliptical pattern. **(D)** Over-impregnated specimen packed with many extrusomes (arrowheads). **(E)** Optical section of the cell periphery showing resting extrusomes. **(F, G)** Extruded extrusomes up to 13 × 0.4 µm long, drumstick-shaped, and slightly curved with a filiform posterior portion **(G)**. **(H–J)** Oral apparatus in three specimens showing the three peniculi (P1, 2, 3), the three vestibular kineties with the rightmost one extending beyond the vestibular cavity, and the paroral membrane. Somatic kineties, the leftmost out of the three vestibular kineties, and the postoral kineties abut on the postoral suture. AS, anterior (preoral) suture; C, cytostome; F, fibers, MA, macronucleus; P1, 2, 3, peniculi; PK, postoral kineties; PM, paroral membrane; PS, postoral suture; VK, vestibular kineties; V, vestibulum. Scale bars: 50 µm **(A, D, J)**, 30 µm **(H, I)**, 15 µm **(B, C)**, and 3.5 µm **(E, G)**.

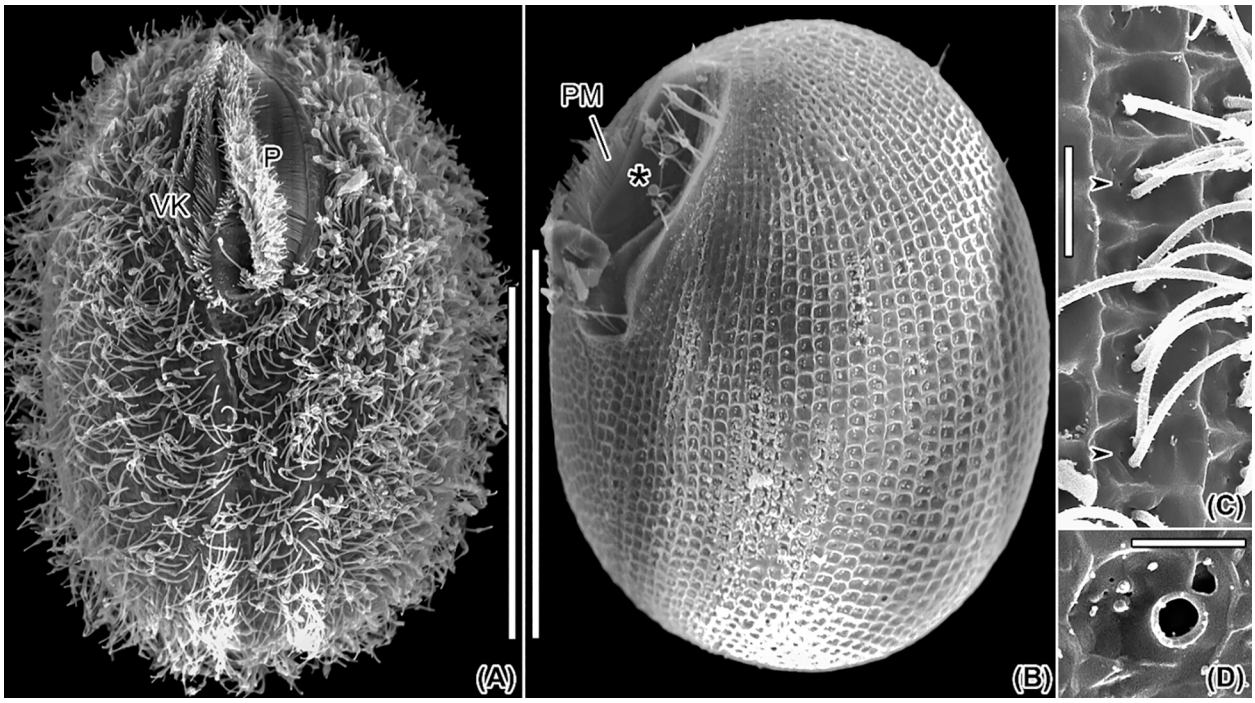

FIGURE 6
Scanning electron micrographs of *Apofrontonia jejuensis* n. sp. **(A)** Ventral view of a representative specimen. **(B)** Ventrolateral view of a deciliated specimen showing the somatic cortical pattern consisting of ordinary peniculine units, i.e., quadrangular meshes. Note that the vestibular cavity is deepest in its anterior half. The oral ribs (associated with the underlying fibrous plate) between paroral membrane and cytostome are exposed (asterisk). **(C)** Surface view in middle portion of left side showing some of the quadrangular meshes with one or two cilia each and a tiny pore likely associated with parasomal sac attachment sites (arrowheads). **(D)** Detail of the excretory pore of a contractile vacuole located between two ciliary rows. P, peniculi; PM, paroral membrane; VK, vestibular kineties. Scale bars: 50 µm **(A, B)** and 2.5 µm **(C, D)**.

Phylogenetic analysis

The 18S rRNA gene sequence of *A. jejuensis* n. sp. is 1,728 base pairs long and has a GC content of 44.38%; it has been deposited under the GenBank accession number OP798095. The genus *Apofrontonia* contains four species, *A. obtusa*, *A. lametschwandtneri*, *A. dohrni*, and *A. jejuensis* n. sp.; however, 18S rRNA gene sequences are only available for the latter two taxa. The ML genealogy was in general congruent with that from the BI analysis, and thus we show here only the ML tree with node support values from both methods (Figure 8). *Apofrontonia jejuensis* n. sp. is sister to *A. dohrni* with full support (100% ML, 1.00 BI), forming the adelphotaxon to a group of seven *Frontonia* species (see below); this cluster is in turn the sister group to a clade of *Paramecium* species (100% ML, 1.00 BI). The sequences of both *Apofrontonia* species have a similarity of 98.1%, differing in 29 nucleotides (Table 2).

The phylogenetic analyses suggest that the family Frontoniidae is paraphyletic (Figure 8), which is consistent with previous publications (Andreoli et al., 2007; Fan et al., 2011; Xu et al., 2018; Li et al., 2022). *Frontonia* species were distributed among three clades in the ML and BI trees (this study; Li et al., 2022): (i) seven species, namely, *Frontonia anatolica* Yildiz and Şenler, 2013, *Frontonia apoelegans* Li et al., 2022, *Frontonia didieri* Long et al., 2008, *Frontonia elegans* Fan et al., 2013, *Frontonia fusca* (Quennerstedt, 1869) Kahl, 1931, "*Frontonia ocularis*" Bullington, 1939, and *Frontonia pusilla* Fan et al., 2013, grouped with the genus *Apofrontonia* (see above); (ii) 14 species [*Frontonia canadensis* Roque and de Puytorac, 1972, *Frontonia leucas* (Ehrenberg, 1833) Ehrenberg, 1838, *Frontonia lynni* Long et al., 2005, *Frontonia magna* Fan et al., 2011, *Frontonia mengi* Fan et al., 2011, *Frontonia paramagna* Chen et al., 2014, *Frontonia paravernalis* Serra et al., 2021, *Frontonia salmastra* Dragesco and Dragesco-Kernéis, 1986, *Frontonia shii* Cai et al., 2018, *Frontonia sinica* Fan et al., 2013, *Frontonia subtropica* Pan et al., 2013, *Frontonia tchibisovae* Burkovsky, 1970, *Frontonia vernalis* (Ehrenberg, 1833) Ehrenberg, 1838, and *Frontonia vesiculosa* Cunha, 1913] form a fully supported clade (100% ML, 1.00 BI) as an adelphotaxon to the grouping of the previously mentioned *Frontonia* species, *Apofrontonia*, and *Paramecium*; and (iii) five species, namely, *Frontonia acuminata*, *Frontonia apoacuminata* Li et al., 2021, *Frontonia atra* (Ehrenberg, 1833) Bütschli, 1889, *Frontonia minuta* Dragesco, 1970, and *Frontonia terricola* Foissner, 1987, are a sister group to the family Stokesiidae (genera *Disematostoma*, *Marituja*, and *Stokesia*). The sequence identities and nucleotide differences among the *Frontonia* species, *Marituja* cf. *caudata*, *Disematostoma minor* Kahl, 1931, and the *Apofrontonia* species are displayed in Table 2.

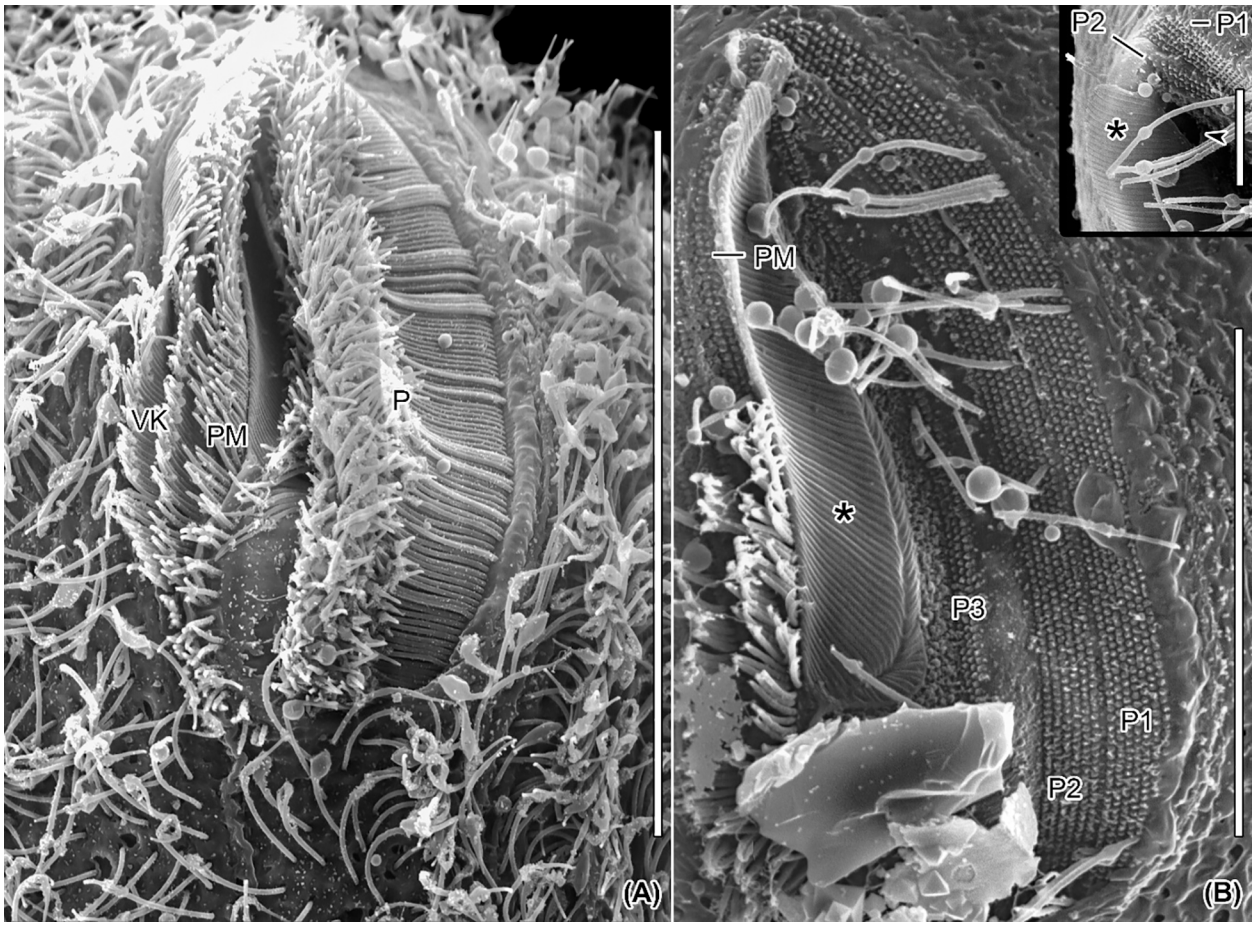

FIGURE 7
Scanning electron micrographs of *Apofrontonia jejuensis* n. sp. Ventral views of the vestibular cavity in one ciliated **(A)** and one artificially unciliated **(B)** specimen. **(A)** The deepest point of the vestibular cavity is in its anterior half. The long cilia of peniculus 3 covers those of peniculi 1 and 2. The paroral membrane extends left of the three vestibular kineties. **(B)** Invariably, the peniculi (P1/P2/P3) comprise seven, six, and three basal body rows, respectively. Oral ribs (associated with the underlying fibrous plate) extend between the paroral membrane and the cytostome (asterisk). The inset shows a detailed view of the main picture, i.e., the anterior end of the vestibular cavity. P1, 2, 3, peniculi; PM, paroral membrane; VK, vestibular kineties. Scale bars: 35 µm **(A)**, 20 µm **(B)**, and 5 µm (inset).

Discussion

Comparison with related species

The morphological differences between *Apofrontonia jejuensis* n. sp. and its congeners *A. dohrni*, *A. lametschwandtneri*, and *A. obtusa* are summarized in the Supplementary Table S1.

Apofrontonia jejuensis n. sp. has a smaller size *in vivo* than *A. lametschwandtneri* (180 × 120 µm) and *A. dohrni* (135 × 65 µm). *Apofrontonia jejuensis* n. sp. differs from the similarly sized *A. obtusa* mainly in the habitat (marine vs. freshwater); further differences between these two species are: (i) the ratio of vestibulum length to body length (0.4 vs. 0.5–0.75), (ii) the macronucleus shape and size (125 × 5 µm in size, horseshoe-shaped with ends sometimes almost meeting one another or crossing over each other vs. approximately <100 × 25 µm in size, compact, sausage-shaped), (iii) the number (1–3 vs. 1) and position (distant from macronucleus and near posterior body end vs. adjacent to macronucleus) of micronuclei, (iv) number of somatic kineties (78 vs. 90), (v) the number of the contractile vacuoles (approximately 20 vs. 4–5), (vi) the number of vestibular kineties (3 vs. 9–10), and (vii) the number of postoral kineties (2–9 vs. none) (Song and Wilbert, 1989; Foissner and Song, 2002; Fokin et al., 2006).

The oral ciliature varies among *Apofrontonia* species, e.g., in the number of vestibular kineties (3 in *A. jejuensis* n. sp.; 4 in *A. dohrni*; 9 in *A. obtusa*; and 13 in *A. lametschwandtneri*). In contrast to its congeners, the rightmost vestibular kinety of *A. jejuensis* n. sp. extends beyond the posterior end of the vestibular cavity. The numbers of ciliary rows in the three peniculi (P1/P2/P3) are also species-specific: 13, 10, and 4 in *A. lametschwandtneri*; 5 or 6, 4 or 5, and 3 in *A. dohrni*; 7, 6, and 3 in *A. jejuensis* n. sp.; and 6, 6, and 3 or 4 in *A. obtusa* (Song and Wilbert, 1989; Foissner and Song, 2002; Fokin et al., 2006).

The term postoral kinety is subject to different interpretations in the genus *Apofrontonia*. For instance, Foissner and Song (2002) described 10 postoral kineties in the type species *A. lametschwandtneri*; however, they did not include this character

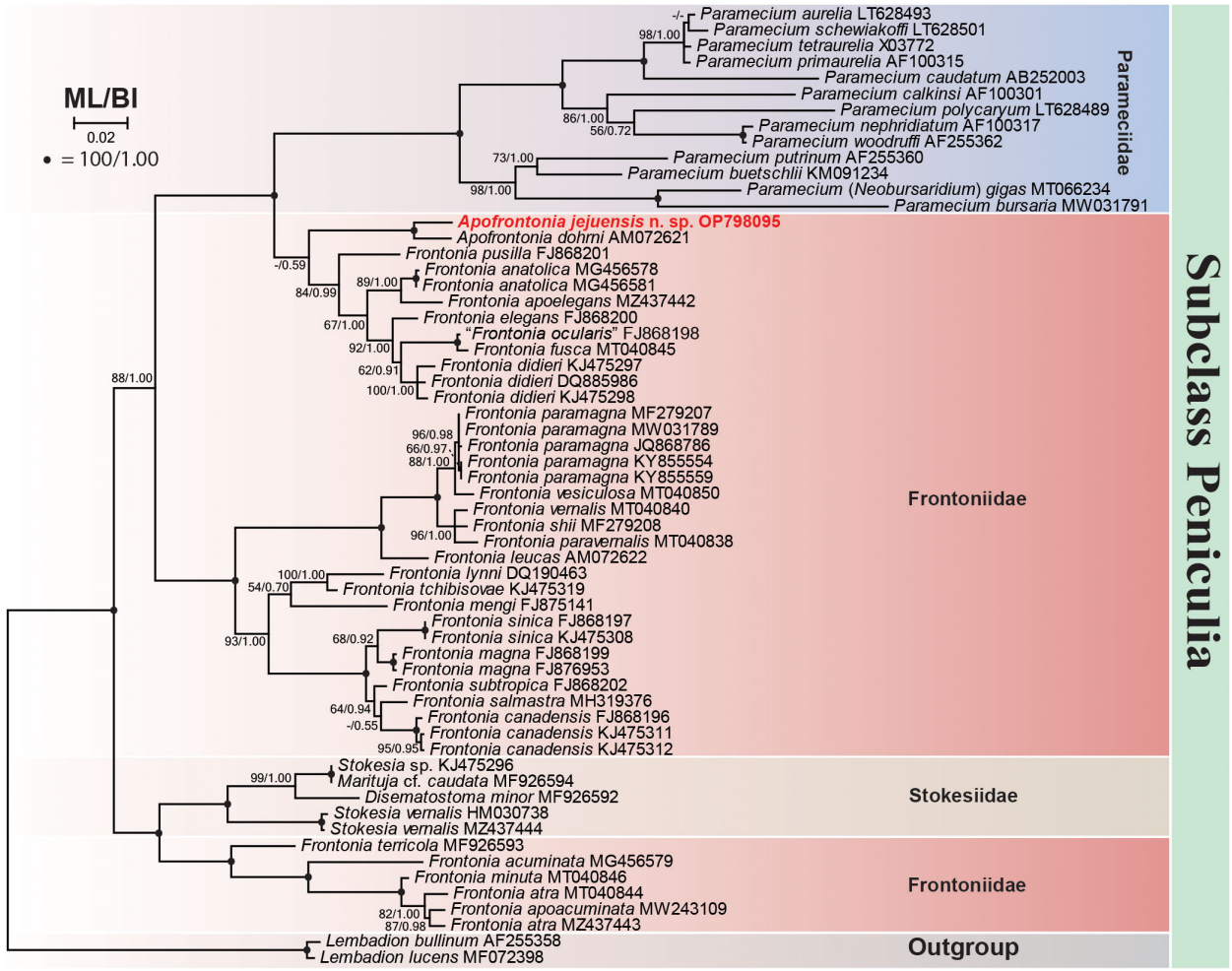

FIGURE 8
Maximum likelihood (ML) phylogenetic tree inferred from the 18S rRNA gene sequences showing the position of *Apofrontonia jejuensis* n. sp. (bold red). Support values are given at the respective nodes as maximum likelihood (ML) bootstrap percentages out of 1,000 replicates/Bayesian inference (BI) posterior probabilities. The dash lines indicate a different topology in BI and ML phylogenies. GenBank accession numbers follow the species names. The scale bar corresponds to two substitutions per 100 nucleotide positions. Note that *"Frontonia ocularis"* (FJ868198) was considered as a junior synonym of *Frontonia fusca* by Serra et al. (2021).

in the genus diagnosis. Based on their line drawings (see Figures 12, 18, and 19, page 228), it is difficult to infer how they defined "postoral kineties" particularly as the authors did not label them. Apparently, they regarded all kineties that are anteriorly shortened and thus do not commence at the preoral suture as postoral kineties. Fokin et al. (2006) reported that both *A. lametschwandtneri* and *A. dohrni* lack postoral kineties and included this feature into the genus diagnosis. Probably, these authors applied the term "postoral" *sensu* Lynn (2008), i.e., placed below the posterior border of the vestibular cavity. According to the latter approach, *A. dohrni* lacks postoral kineties, since the elongated and narrow posterior end of the vestibular cavity prevents the occurrence of a postoral field. However, our hypothesis concerning Foissner and Song (2002)'s interpretation of the postoral kineties should be applied to *A. dohrni*, which could present such structures, although unfortunately they cannot be clearly detected in the published line drawings and photomicrographs (see Figures 2b and 3a, pages 293 and 294, respectively, in Fokin et al., 2006). The description of *A. obtusa* (basionym: *F. obtusa* Song and Wilbert, 1989) does not mention any postoral kineties, while the line drawing shows at least two short rows posterior to the vestibular cavity (see Figure 57d, page 110). Thus, a reinvestigation of the type slides of these *Apofrontonia* species is needed to confirm their descriptions and shed light on this discussion. *Apofrontonia jejuensis* n. sp. is most similar to *A. lametschwandtneri* in having postoral kineties abutting on the postoral suture posteriorly, including both some *sensu* Lynn (2008) (i.e., terminating anteriorly at the posterior border of the vestibular cavity) and some *sensu* Foissner and Song (2002) postoral kineties (i.e., terminating anteriorly along the left vestibular border).

Foissner and Song (2002) distinguished *Apofrontonia* from *Frontonia* and *Disematostoma* based on the absence (vs. presence) of a postoral field, which hides the posterior portion of the peniculi in *Frontonia* and *Disematostoma*. In *A. lametschwandtneri*, the

TABLE 2 Sequence similarity (below diagonal) and nucleotide difference (above diagonal) based on 18S rRNA gene sequences among *Apofrontonia jejuensis* n. sp., *Apofrontonia dohrni* (AM072621), *Disematostoma minor* (MF926592), *Frontonia anatolica* (MG456578), *Frontonia apoelegans* (MZ437442), *Frontonia didieri* (KJ475297), *Frontonia elegans* (FJ868200), *Frontonia fusca* (MT040845), *Frontonia leucas* (AM072622), *Frontonia magna* (FJ876953), "*Frontonia ocularis*" (FJ868198, considered as a junior synonym of *F. fusca* by Serra et al., 2021), *Frontonia pusilla* (FJ868201), *Lembadion lucens* (MF072398), *Marituja* cf. *caudata* (MF926594), *Paramecium aurelia* (LT628493), and *Stokesia vernalis* (HM030738).

Species	1	2	3	4	5	6	7	8	9	10	11	12	13	14	15	16
1- Apofrontonia jejuensis n. sp.	–	29	77	90	75	86	83	84	141	87	132	144	179	137	152	140
2- *Apofrontonia dohrni*	0.981	–	84	89	79	89	82	89	142	91	132	152	178	146	153	145
3- *Frontonia anatolica*	0.951	0.946	–	23	47	45	38	49	143	48	127	137	175	134	133	138
4- *Frontonia apoelegans*	0.942	0.943	0.985	–	48	56	49	53	145	53	130	138	178	136	137	142
5- *Frontonia pusilla*	0.952	0.949	0.970	0.969	–	58	53	63	145	66	135	153	177	144	146	144
6- *Frontonia didieri*	0.945	0.943	0.971	0.964	0.963	–	25	40	146	37	141	159	188	147	142	147
7- *Frontonia elegans*	0.947	0.947	0.975	0.968	0.966	0.984	–	38	138	35	131	154	184	140	144	144
8- *Frontonia fusca*	0.946	0.943	0.968	0.966	0.959	0.974	0.975	–	150	5	139	151	193	140	148	146
9- *Frontonia leucas*	0.910	0.909	0.909	0.907	0.907	0.907	0.912	0.904	–	151	100	150	168	140	167	133
10- *Frontonia ocularis*	0.944	0.942	0.969	0.966	0.958	0.976	0.977	0.996	0.907	–	140	151	192	139	148	143
11- *Frontonia magna*	0.916	0.916	0.919	0.917	0.914	0.910	0.916	0.911	0.936	0.911	–	140	158	135	169	133
12- *Disematostoma minor*	0.908	0.903	0.912	0.912	0.902	0.898	0.902	0.904	0.904	0.904	0.910	–	168	45	165	81
13- *Lembadion lucens*	0.886	0.887	0.888	0.887	0.887	0.880	0.883	0.877	0.893	0.878	0.899	0.893	–	160	199	166
14- *Marituja* cf. *caudata*	0.912	0.907	0.914	0.913	0.908	0.906	0.911	0.911	0.910	0.911	0.914	0.971	0.898	–	163	70
15- *Paramecium aurelia*	0.903	0.902	0.915	0.912	0.907	0.909	0.908	0.906	0.893	0.906	0.892	0.895	0.873	0.896	–	163
16- *Stokesia vernalis*	0.910	0.907	0.912	0.909	0.908	0.906	0.908	0.907	0.915	0.909	0.915	0.948	0.894	0.955	0.8s6	–

10.3389/fmars.2023.1216564

authors interpreted the exposure of the entire peniculi by the absence of a postoral field despite the presence of postoral kineties (as defined by Lynn, 2008) and used this character in the diagnosis of the genus. The new species, *A. jejuensis* n. sp., shows a similar morphology but with a higher number of postoral kineties *sensu* Lynn (2008), indicating that the postoral field of *A. lametschwandtneri* is in fact present but highly reduced.

According to Lynn (2008), nematodesma (pl. nematodesmata) is a "birefringent bundle of parallel microtubules often showing a hexagonal, paracrystalline arrangement in cross section; typically, kinetosome-associated; plunging into the cytoplasm at right angles to the pellicle, forming with others the major reinforcements of the cytopharyngeal apparatus" (page 39). Although different silver staining methods or differential interference contrast may sometimes reveal nematodesmata, their presence can only be confirmed by transmission electron microscopy. Nematodesmata are common in different ciliate groups, including haptorians, nassophoreans, cyrtophoreans or frontoniids, among others (Lynn, 2008). However, their presence in *Apofrontonia* species has neither been mentioned (original descriptions of *A. obtusa* and *A. lametschwandtneri*) nor been observed (*A. dohrni*). Fokin et al. (2006) argued that nematodesmata are visible in living specimens of *Frontonia* species using differential interference contrast microscopy and they are too distinct to be overlooked in *Apofrontonia* if they would really be present. Consequently, they considered that any of the previously mentioned *Frontonia* species possesses nematodesmata. Although oral nematodesmata are a distinguishing character of the family Frontoniidae (de Puytorac et al., 1987; Lynn, 2008), it is well known that their distinctness varies among congeners, e.g., the nematodesmata of *F. fusca* (Quennerstedt, 1869) Kahl, 1931, are weakly developed compared to those of congeners (Foissner et al., 1994; Foissner et al., 2002; Fokin, 2008). *Apofrontonia jejuensis* n. sp. shows a fibrillar system associated with the oral ciliature, which is partially visible *in vivo*, using differential interference contrast but more distinct after application of silver staining methods. We assume that this fibrillar system might represent the nematodesmata-like structures as those found in *Frontonia* species; however, verification necessitates the application of transmission electron microscopy, which unfortunately has been used in neither the previous nor the present descriptions of *Apofrontonia* species. As yet, *A. jejuensis* n. sp. is the only species displaying such a fibrillar system, but its presence in the congeners is very likely where it might be more poorly developed or stained. Efforts should be made to increase the taxon sampling within the family Frontoniidae, providing additional phylogenetic and morphological/ultrastructural information. Furthermore, the application of transmission electron microscopy could contribute to the improvement of the taxon diagnoses.

Comparison with related genera

The conspicuous oral apparatus distinguishes the genera *Apofrontonia* and *Lembadion* and the subgenus *Neobursaridium* of *Paramecium* (Serra, et al., 2020; Serra et al., 2022) from the other peniculines. These taxa can be easily separated because of their distinctive morphology (e.g., *Lembadion* and *Neobursaridium* lack vestibular kineties, etc.) and phylogenetic placements.

Previous morphological and genetic studies indicate that the genera *Frontonia* and *Marituja* are the closest relatives of *Apofrontonia* (Foissner and Song, 2002; Fokin et al., 2006); however, the latter genus differs from *Marituja* in the orientation of somatic ciliary rows (longitudinal vs. transverse/"circular") (Gajewskaja, 1928; Wilbert, 1972; Foissner et al., 1999; Xu et al., 2018). *Apofrontonia* differs from *Frontonia* in (i) the length of the vestibular kineties (rarely extending beyond the vestibular cavity vs. extending postorally and abutting on the postoral suture), (ii) the shape of the vestibular opening (bean-shaped, pyriform or key-hole-shaped vs. triangular or fusiform), (iii) the posterior part of the bowl-shaped vestibulum (gradually merging into the cell surface, completely exposing the posterior portions of the peniculi vs. the posterior portions of the peniculi are covered by a triangular postoral field) (Foissner and Song, 2002; Fokin et al., 2006). The new data on *A. jejuensis* n. sp., together with a detailed study of the descriptions, drawings, and micrographs from previous studies of other related species, shed light on different unknown or poorly described morphological features of the genus *Apofrontonia* as originally described by Foissner and Song (2002). Thus, thanks to these new findings, we provide an improved diagnosis of the genus, mainly including (i) the presence of a postoral field, which can be highly reduced in some species, but regardless of whether it is reduced or not, it does not cover the posterior end of the peniculi; (ii) the presence of postoral kineties following the interpretation of Foissner and Song (2002), i.e., kineties anteriorly terminating below the posterior border of the vestibular cavity and/or terminating left to vestibular margin; (iii) the presence of an argyrophilic plate of nematodesmata-like fibers between the paroral membrane and cytostome; and (iv) a great range of salinity tolerance within aquatic and terrestrial habitats.

Our molecular analyses of the genus *Frontonia* match those of Sun et al. (2020) and Li et al. (2022) in the presence of three clusters: (i) the core cluster consisting of 14 *Frontonia* species, including the type species *F. leucas* (Ehrenberg, 1833) Ehrenberg, 1838; (ii) the cluster of seven *Frontonia* species grouping *A. jejuensis* n. sp. and *A. dohrni* as sister to the family Parameciidae; and (iii) the cluster of five species forming a sister group to the family Stokesiidae. However, despite these data supporting the distinctness of the particular clades, we are refraining from splitting the genus *Frontonia* until further morphological and/or ultrastructural studies can define important characters (plesiomorphies and synapomorphies) and resolve the non-monophyly issue of the genus.

Biogeographical considerations

The limited availability of large reliable datasets on the geographic distribution of ciliates primarily focuses on terrestrial biota (Foissner et al., 2008). The existing knowledge gap regarding

the ecological significance and biogeographic patterns of marine ciliates highlights the necessity for additional research to enhance our understanding in this field (Ganser et al., 2021). The geographic distribution of species within the genus *Apofrontonia* is just another example of the complexity of biogeographical studies in protists and how the undersampling drastically limits our knowledge about their biogeographies. In this regard, *Paramecium* spp. present a compelling case study that highlights the challenges associated with comprehending the diversity and biogeographic patterns of ciliate species (Catania et al., 2009; De Souza et al., 2020; Melekhin et al., 2022). *Paramecium* has provided valuable insights revealing that speciation does not strictly conform to cladistic principles. Furthermore, it has suggested the possibility of cyclical and rapid transitions from a geographically limited distribution to a temporary and cosmopolitan distribution (Catania et al., 2009). Additionally, *Paramecium* has shed light on the extensive diversity of cryptic species within recognized taxa, surpassing previous assumptions (De Souza et al., 2020). Contrary to *Paramecium* spp., *Apofrontonia* spp. have only recently been discovered, despite being conspicuous ciliates. This observation suggests their rarity. In fact, the genus was established by Foissner and Song (2002) after the discovery of *A. lametschwandtneri* and also includes *A. obtusa*, the basionym of *F. obtusa* Song and Wilbert, 1989. All known *Apofrontonia* species are morphologically similar but exhibit different habitat preferences (*A. obtusa* inhabits freshwater ponds, *A. dohrni* and *A. lametschwandtneri* can be found in mud from coastline puddles, and *A. jejuensis* n. sp. is present in coastal waters), and their biogeographical distribution is restricted for now to widely separated geographic regions (*A. obtusa* in Germany, *A. dohrni* in Italy, *A. lametschwandtneri* in Venezuela, and *A. jejuensis* n. sp. in South Korea) (Foissner et al., 2008). However, due to the fact that some species within the genus, namely, *A. dohrni* and *A. fusca*, can tolerate euryhaline conditions, ranging from 1‰ to 18‰ and from 4‰ to 25‰, respectively (Fokin et al., 2006; Fokin, 2008), it cannot be excluded that the genus *Apofrontonia* could have a much wider biogeographical species distribution than currently known. Additionally, the occurrence of syngens in *Apofrontonia*, reproductively isolated groups, as it is known for *Paramecium* morphospecies (Sonneborn, 1975; Potekhin and Mayén-Estrada, 2020; Melekhin et al., 2022), remains unknown for now until new morphological and molecular studies could increase the taxon sampling within the genus.

This study constitutes a modest contribution to our comprehension of biogeographic aspects associated with peniculine ciliates, representing a step forward in understanding their distribution and speciation patterns. However, there is still much to uncover and explore in our understanding of the effective dispersal capabilities of ciliates, particularly those associated with marine environments.

Data availability statement

The datasets presented in this study can be found in online repositories. The names of the repository/repositories and accession number(s) can be found in the article/Supplementary Material.

Author contributions

PQ-A, AO, and J-HJ designed the study and revised the article. All authors performed morphological experiments, molecular experiments, and data analyses and wrote the article. JHM collected the samples and helped in the scanning electron microscopy. All authors read and approved the final version of the article.

Funding

This research was supported by the management of Marine Fishery Bio-resources Center (2023) funded by the National Marine Biodiversity Institute of Korea (MABIK).

Acknowledgments

We would like to express our sincere gratitude to two reviewers for their invaluable input and insightful comments. We are grateful to the Center for Research Facilities at Gangneung-Wonju National University for their assistance in the analysis of the cell structure (CPD, SEM, etc.).

Conflict of interest

The authors declare that the research was conducted in the absence of any commercial or financial relationships that could be construed as a potential conflict of interest.

Publisher's note

Supplementary material

The Supplementary Material for this article can be found online at: https://www.frontiersin.org/articles/10.3389/fmars.2023.1216564/full#supplementary-material

References

Andreoli, I., Fokin, S. I., Verni, F., and Petroni, G. (2007). Phylogenetic relationships within peniculine ciliates and the paraphyly of *Frontonia*. *Protistology* 5, 12.

Borror, A. C. (1963). Morphology and ecology of the benthic ciliated protozoa of Alligator Harbor. Florida. *Arch. Protistenk.* 106, 465–534.

Bullington, W. E. (1939). A study of spiraling in the ciliate *Frontonia* with a review of the genus and a description of two new species. *Arch. Protistenk.* 92, 10–66.

Burkovsky, I. V. (1970). The ciliates of the mesopsammon of the kandalaksha gulf (White sea) II. *Acta Protozool.* 8, 47–65.

Bütschli, O. (1889). "Protozoa III. abtheilung: Infusoria und system der radiolaria," in *Klassen und ordnungen des thier-reichs, wissenschaftlich dargestellt in wort und bild*, vol. I . Ed. „. H. G. Bronn (Winter, Leipzig: Tafeln LVI-LXXIX), 1585–2035.

Cai, X., Wang, C., Pan, X., El-Serehy, H. A., Mu, W., Gao, F., et al. (2018). Morphology and systematics of two freshwater *Frontonia* species (Ciliophora, peniculida) from northeastern china, with comparisons among the freshwater frontonia spp. *Eur. J. Protistol.* 63, 105–116. doi: 10.1016/j.ejop.2018.01.002

Catania, F., Wurmser, F., Potekhin, A. A., Przybos, E., and Lynch, M. (2009). Genetic diversity in the *Paramecium aurelia* species complex. *Mol. Biol. Evol.* 26, 421–431. doi: 10.1093/molbev/msn266

Chen, Y., Zhao, Y., Pan, X., Ding, W., Al-Rasheid, K. A. S., and Qiu, Z. (2014). Morphology and phylogeny of a new *Frontonia* ciliate, *F. paramagna* spec. nov. (Ciliophora, peniculida) from harbin, northeast china. *Zootaxa.* 3827, 375–386. doi: 10.11646/zootaxa.3827.3.7

Corliss, J. O. (1956). On the evolution and systematics of ciliated protozoa. *Syst. Zool.* 5, 121–140. doi: 10.2307/2411574

Corliss, J. O. (1979). *The ciliated protozoa: Characterization, classification, and guide to the literature. 2nd edition* (London/New York: Pergamon Press), 1–455.

Cunha, A. M. (1913). Contribuição para o conhecimento da fauna de protozoarios do brazil (Beitraege zur kenntnis der protozoenfauna brasiliens). *Mems Inst. Oswaldo Cntz* 5, 101–122.

Darriba, D., Taboada, G. L., Doallo, R., and Posada, D. (2012). jModelTest 2: more models, new heuristics and parallel computing. *Nat. Methods* 9, 772. doi: 10.1038/nmeth.2109

de Puytorac, P., Grain, J., and Mignot, J. P. (1987). *Précis de Protistologie* (Boubée: Soc. Nouv. Ed. Paris), 581.

de Puytorac, P., Batisse, A., Bohatier, J., Corliss, J. O., Deroux, G., Didier, P., et al. (1974). Proposition d'une classification du phylum ciliophora doflei. *Compt. Rend. Acad. Sci.,Paris.* 278, 2799–2802.

De Souza, B. A., Dias, R. J. P., and Senra, M. V. X. (2020). Intrageneric evolutionary timing and hidden genetic diversity of Paramecium lineages (Ciliophora: Oligohymenophorea). *Syst. Biodivers.* 18, 662–674. doi: 10.1080/14772000.2020.1769225

Dragesco, J. (1960). "Ciliés mésopsammiques littoraux, systématique, morphologie, écologie," in *Travaux de la Station biologique de Roscoff (Nouvelle Serie), tome XII*, vol. 12. (Paris: Presses Universitaires de France), 1–356.

Dragesco, J. (1970). Ciliés libres du Cameroun. *Annls. Fac. Sci. Univ. fed. Cameroun (Numero hors-serie*), 1–141.

Dragesco, J. (1972). Ciliés libres de l'Ouganda. *Annales la Faculte Des. Sci. du Cameroun.* 9, 87–126.

Dragesco, J., and Dragesco-Kernéis, A. (1986). Ciliés libres de l'Afrique intertropicale. Introduction à la connaissance et à l'étude des ciliés. *Faune Trop.* 26, 1–559.

Dujardin, F. (1840). Memoire sur une classification des infusoires en rapport avec leur organisation.- c. *R. hebd. Séanc. Acad. Sci. Paris* 11, 281–286.

Ehrenberg, C. G. (1838). Die infusionsthierchen als vollkommene organismen. ein blick in das tiefere organische leben der natur. *L. Voss Leipzig* 4, 1–612, 64 Pl.

Fan, X., Chen, X., Song, W., Al-Rasheid, K. A. S., and Warren, A. (2011). Two novel marine *Frontonia* species, *Frontonia mengi* spec. nov. and *Frontonia magna* spec. nov. (Protozoa; Ciliophora), with notes on their phylogeny based on small-subunit rDNA gene sequence data. *Int. J. Syst. Evol. Microbiol.* 61, 1476–1486. doi: 10.1099/ijs.0.024794-0

Fan, X., Li, X., Li, W., Xu, Y., Al-Farraj, S. A., Al-Rasheid, K. A. S., et al. (2013). Morphology of three new marine *Frontonia* species (Ciliophora; Peniculida) with note on the phylogeny of this genus. *Eur. J. Protistol.* 49, 312–323. doi: 10.1016/j.ejop.2012.06.003

Foissner, W. (1991). Basic light and scanning electron microscopic methods for taxonomic studies of ciliated protozoa. *Eur. J. Protistol.* 27, 313–330. doi: 10.1016/S0932-4739(11)80248-8

Foissner, W. (2014). An update of 'basic light and scanning electron microscopic methods for taxonomic studies of ciliated protozoa'. *Int. J. Syst. Evol. Microbiol.* 64, 271–292. doi: 10.1016/S0932-4739(11)80248-8

Foissner, W., Agatha, S., and Berger, H. (2002). Soil ciliates (Protozoa, Ciliophora) from Namibia (Southwest Africa), with emphasis on two contrasting environments, the Etosha region and the Namib desert. *Denisia* 5, 1–1459.

Foissner, W., Berger, H., and Kohmann, F. (1994). Taxonomische und ökologische Revision der Ciliaten des Saprobiensystems – Band III: Hymenostomata, Prostomatida, Nassulida. *Informationsberichte Des. Bayerischen Landesamtes für Wasserwirtschaft* 1/94, 1–548.

Foissner, W., Berger, H., and Schaumburg, J. (1999). *Identification and ecology of limnetic plankton ciliates. Informationsberichte des Bayer* Vol. 3/99 (Munich: Landesamtes Wasserwirtsch), 793.

Foissner, W., Chao, A., and Katz, L. A. (2008). Diversity and geographic distribution of ciliates (Protista: Ciliophora). *Biodivers. Conserv.* 17, 345–363. doi: 10.1007/s10531-007-9254-7

Foissner, W., and Song, W. (2002). *Apofrontonia lametschwandtneri* nov. gen., nov. spec., a new peniculine ciliate (Protozoa, Ciliophora) from Venezuela. *Eur. J. Protistol.* 38, 223–234. doi: 10.1078/0932-4739-00870

Foissner, W. (1987). Neue terrestrische und limnische ciliaten (Protozoa, ciliophora) aus Österreich und deutschland. *Sber. Akad. Wiss. Wien* 195, 217–268.

Fokin, S. (2008). Rediscovery and characterisation of *Frontonia fusca* (Quennerstedt 1869) Kahl 1931 (Ciliophora, Peniculia). *Denisia* 23, 251–259.

Fokin, S., Andreoli, I., Verni, F., and Petroni, G. (2006). *Apofrontonia dohrni* sp. n. and the phylogenetic relationships within Peniculia (Protista, Ciliophora, Oligohymenophorea). *Zool. Scr.* 35, 289–300. doi: 10.1111/j.1463-6409.2006.00231.x

Gajewskaja, N. (1928). Sur quelques infusoires pelagiques nouveaux du lac Baikal. *Dokl. Akad. nauk SSSR* 20, 476–478.

Ganser, M. H., Forster, D., Liu, W., Lin, X., Stoeck, T., and Agatha, S. (2021). Genetic diversity in marine planktonic ciliates (Alveolata, Ciliophora) suggests distinct geographical patterns – data from Chinese and European coastal waters. *Front. Mar. Sci.* 8. doi: 10.3389/fmars.2021.643822

Gao, F., Warren, A., Zhang, Q., Gong, J., Miao, M., Sun, P., et al. (2016). The all-data-based evolutionary hypothesis of ciliated protists with a revised classification of the Phylum ciliophora (Eukaryota, Alveolata). *Sci. Rep.* 6, 24874. doi: 10.1038/srep24874

Gil, R., and Perez-Silva, J. (1964a). The infraciliature of *Frontonia depressa* Stokes. *Arch. Protistenk.* 107, 363–372.

Gil, R., and Perez-Silva, J. (1964b). La infraciliación de *Frontonia leucas* Ehrenberg. *Microbiol. Esp.* 17, 239–254.

Gil, R., and Perez-Silva, J. (1964c). La infraciliación de *Frontonia acuminata* Ehrenberg. *Microbiol. Esp.* 17, 69–77.

Hall, T. A. (1999). BioEdit: a user-friendly biological sequence alignment editor and analysis program for Windows 95/98/ NT. *Nucleic Acids Symp. Ser.* 41, 95–98.

Jung, J.-H., and Min, G.-S. (2009). New record of two species in stichotrichous ciliates (Ciliophora: Stichotrichia) from Korea. *Korean J. Systematic Zoology* 25, 227–236. doi: 10.5635/KJSZ.2009.25.3.227

Jung, J.-H., Moon, J. H., Park, K.-M., Kim, S., Dolan, J. R., and Yang, E. J. (2018). Novel insights into the genetic diversity of *Parafavella* based on mitochondrial CO1 sequences. *Zool. Scr.* 47, 743–755. doi: 10.1111/zsc.12312

Kahl, A. (1926). Neue und wenig bekannte formen der holotrichen und heterotrichen ciliaten. *Arch. Protistenk.* 55, 197–438.

Kahl, A. (1931). *Urtiere order Protozoa I: Wimpertiere order Ciliata (Infusoria) 2. Holotricha außer denim 1. Teil behandelten Prostomata* Vol. 21 (Germany: Tierwelt Dtl), 181–398.

Kearse, M., Moir, R., Wilson, A., Stones-Havas, S., Cheung, M., Sturrock, S., et al. (2012). Geneious Basic: an integrated and extendable desktop software platform for the organization and analysis of sequence data. *Bioinformatics* 28, 1647–1649. doi: 10.1093/bioinformatics/bts199

Kim, J. H., and Jung, J.-H. (2017). Cytological staining of protozoa: a case study on the impregnation of hypotrichs (Ciliophora: spirotrichea) using laboratory-synthesized protargol. *Anim. Cells Syst.* 21, 412–418. doi: 10.1080/19768354.2017.1376707

Lauterborn, R. (1894). Ueber die winterfauna einiger gewasser der oberrheinebene. mit beschreibungen neuer protozoen. *Bioi. Zbl.* 14, 390–398.

Li, T., Liu, M., Warren, A., Al-Farraj, S. A., Yi, Z., and Sheng, Y. (2022). Morphology and SSU rRNA gene-based phylogeny of three peniculid ciliates (Ciliophora, Oligohymenophorea) from China, including a new *Frontonia* species. *Eur. J. Protistol.* 85, 125910. doi: 10.1016/j.ejop.2022.125910

Li, T., Pan, X. M., Lu, B. R., Miao, M., and Liu, M. J. (2021). Taxonomy and molecular phylogeny of a new freshwater ciliate frontonia apoacuminata sp. nov. (Protista, ciliophora, oligohymenophorea) from qingdao, PR china. *Int. J. Syst. Evol. Microbiol.* 71, 005071. doi: 10.1007/s42995-022-00154-x

Lincoln, R. J., Boxshall, G. A., and Clark, P. F. (1982). *A dictionary of ecology, evolution and systematics* (Cambridge and Sydney: Cambridge Univ. Press), 298.

Long, H., Song, W., Al-Rasheid, K. A. S., Wang, Y., Yi, Z., Al-Quraishy, S. A., et al. (2008). Taxonomic studies on three marine species of *Frontonia* from northern China: *F. didieri* n. sp., *F. multinucleata* n. sp. and *F. tchibisovae* Burkovsky 1970 (Ciliophora: Peniculida). *Zootaxa* 1687, 35–50. doi: 10.5281/zenodo.180528

Long, H., Song, W., Gong, J., Hu, X., Ma, H., Zhu, M., et al. (2005). *Frontonia lynni* n. sp., a new marine ciliate (Protozoa, Ciliophora, Hymenostomatida) from Qingdao, China. *Zootaxa* 1003, 57–64. doi: 10.11646/zootaxa.1003.1.4

Lynn, D. H. (2008). *The ciliated protozoa: characterization, classification and guide to the literature*, *3rd edition* (Dordrecht: Springer), 1–605.

Lynn, D. H., and Small, E. B. (2000). "Phylum ciliophora," in *An illustrated guide to the Protozoa*, *2nd edn*. Eds. J. J. Lee, S. H. Hutner and E. C. Bovee (Lawrence: Allen Press), 371–655.

Medlin, L., Elwood, H. J., Stickel, S., and Sogin, M. L. (1988). The characterization of enzymatically amplified eukaryotic 16S-like rRNA-coding regions. *Gene* 71, 491–499. doi: 10.1016/0378-1119(88)90066-2

Melekhin, M., Yakovleva, Y., Lebedeva, N., Nekrasova, I., Nikitashina, L., Castelli, M., et al. (2022). Cryptic diversity in *Paramecium multimicronucleatum* revealed with a polyphasic approach. *Microorganisms* 10, 974. doi: 10.3390/microorganisms10050974

Moon, J. H., Kim, J. H., Quintela-Alonso, P., and Jung, J.-H. (2020). Morphology, morphogenesis, and molecular phylogeny of *Neobakuella aenigmatica* n. sp. (Ciliophora, Spirotrichea, Bakuellidae). *J. Eukaryot. Microbiol.* 67, 54–65. doi: 10.1111/jeu.12753

Nguyen, L.-T., Schmidt, H. A., von Haeseler, A., and Minh, B. Q. (2015). IQ-TREE: A fast and effective stochastic algorithm for estimating maximum-likelihood phylogenies. *Mol. Biol. Evol.* 32, 268–274. doi: 10.1093/molbev/msu300

Pan, X., Liu, W., Yi, Z., Fan, X., Al-Rasheid, K. A. S., and Lin, X. (2013). Studies on three diverse *Frontonia* species (Ciliophora, Peniculida), with brief notes on 14 marine or brackish congeners. *Acta Protozool.* 52, 35–49. doi: 10.4467/16890027AP.13.004.0832

Park, M.-H., Moon, J. H., Kim, K. N., and Jung, J.-H. (2017). Morphology, morphogenesis, and molecular phylogeny of *Pleurotricha oligocirrata* nov. spec. (Ciliophora: Spirotrichea: StylonyChinae). *Eur. J. Protistol.* 59, 114–123. doi: 10.1016/j.ejop.2017.04.005

Penard, E. (1922). *Études sur les infusoires d'Eau douce* (Genève: Georg and Cie), 1–331. doi: 10.5962/bhl.title.122543

Perty, M. (1849). Über verticale verbreitung mikroskopischer lebensformen. *Mitt. naturf. Ges. Bern* 1849, 17–45.

Potekhin, A., and Mayén-Estrada, R. (2020). *Paramecium* diversity and a new member of the *Paramecium aurelia* species complex described from Mexico. *Diversity* 12, 197. doi: 10.3390/d12050197

Quennerstedt, A. (1869). Bidrag till sveriges infusorie-fauna. III. *Acta Univ. lund.* 6, 1–35.

Rambaut, A. (2006). *FigTree* (Institute of Evolutionary Biology, Univ. of Edinburgh). Available at: http://tree.bio.ed.ac.uk/software/figtree/.

Ronquist, F., Teslenko, M., van der Mark, P., Ayres, D. L., Darling, A., Hohna, S., et al. (2012). MrBayes 3.2: efficient Bayesian phylogenetic inference and model choice across a large model space. *Syst. Biol.* 61, 539–542. doi: 10.1093/sysbio/sys029

Roque, M. (1961). Recherches sur les infusoires ciliés: les hyménostomes péniculiens. *Bull. biologique la France la Belgique* 95, 431–519.

Roque, M., and de Puytorac, P. (1972). *Frontonia canadensis* sp. nov. (Cilié Hyménostome Péniculien). *Le Naturaliste can.* 99, 411–416.

Serra, V., D'Alessandro, A., Nitla, V., Gammuto, L., Modeo, L., Petroni, G., et al. (2021). The neotypification of *Frontonia vernalis* (Ehrenberg 1833) Ehrenberg 1838 and the description of *Frontonia paravernalis* sp. nov. trigger a critical revision of frontoniid systematics. *BMC Zool.* 6, 4. doi: 10.1186/s40850-021-00067-9

Serra, V., Fokin, S. I., Gammuto, L., Nitla, V., Castelli, M., Basuri, C. K., et al. (2020). Phylogeny of Neobursaridium reshapes the systematics of *Paramecium* (Oligohymenophorea, Ciliophora). *Zool. Scr.* 50, 241–268. doi: 10.1111/zsc.12464

Serra, V., Fokin, S. I., Gammuto, L., Nitla, V., Castelli, M., Basuri, C. K., et al. (2022). Phylogeny of *Neobursaridium* reshapes the systematics of *Paramecium* (Oligohymenophorea, Ciliophora). *Zool. Scr.* 51, 478–481. doi: 10.1111/zsc.12529

Small, E. B., and Lynn, D. H. (1985). "Phylum ciliophora doflein 1901," in *An Illustrated Guide to the Protozoa. Society of Protozoologists Special Publication*. Eds. J. J. Lee, S. H. Hutner and E. D. Bovee (Lawrence, Kansas: Allen Press), 393–575.

Song, W. (1995). Studies on the stomatogenesis of *Frontonia acuminata* (Ciliophora, Hymenostomatida). *Acta Hydrobiol. Sin.* 19, 257–262.

Song, W., and Wilbert, N. (1989). Taxonomische untersuchungen an aufwuchciliaten (Protozoa, Ciliophora) im poppelsdorfer weiher, bonn. *Lauterbornia* 3, 2–221.

Sonneborn, T. M. (1975). The *Paramecium-aurelia* complex of 14 sibling species. *Trans. Am. Microsc. Soc* 94, 155–178. doi: 10.2307/3224977

Sun, M., Li., Y., Cai, X., Liu, Y., Chen, Y., and Pan, X. (2020). Further insights into the phylogeny of peniculid ciliates (Ciliophora, Oligohymenophorea) based on multigene data. *Mol. Phylogenet. Evol.* 154, 107003. doi: 10.1016/j.ympev.2020.107003

Tamura, K., Stecher, G., Peterson, D., Filipski, A., and Kumar, S. (2013). MEGA 6: molecular evolutionary genetics analysis version 6.0. *Mol. Biol. Evol.* 30, 2575–2579. doi: 10.1093/molbev/mst197

Thompson, J. D., Higgins, D. G., and Gibson, T. J. (1994). CLUSTAL W: improving the sensitivity of progressive multiple sequence alignment through sequence weighting, position-specific gap penalties and weight matrix choice. *Nucleic Acids Res.* 22, 4673–4680. doi: 10.1093/nar/22.22.4673

Wenrich, D. H. (1929). Observations on some freshwater ciliates (Protozoa). II. *Paradileptus*, n. gen.-. *Trans. Am. microsc. Soc* 48, 352–365.

Wilbert, N. (1972). Die Infraciliatur von *Marituja pelagica* Gajewskaja 1928. *J. Protozool.* 19, 590–592. doi: 10.1111/j.1550-7408.1972.tb03535.x

Xu, Y., Gao, F., and Fan, X. (2018). Reconsideration of the systematics of Peniculida (Protista, Ciliophora) based on SSU rRNA gene sequences and new morphological features of *Marituja* and *Disematostoma*. *Hydrobiologia* 806, 313–331. doi: 10.1007/s10750-017-3371-4

Yildiz, I., and Şenler, N. G. (2013). *Frontonia anatolica* n. sp., a new peniculid ciliate (Protista, ciliophora) from lake van, turkey. *Turk. J. Zool.* 37, 24–30. doi: 10.3906/zoo-1203-33